JOURNAL OF GEOPHYSICAL RESEARCH, VOL. 103, NO. B6, PAGES 12,239-12,260, JUNE 10, 1998

Oxide-metal equilibria to 2500°C and 25 GPa: Implications for core formation and the light component in the Earth's core

Hugh St.C. O'Neill[1]

Research School of Earth Sciences, Australian National University, Canberra , Australia

Dante Canil[2] and David C. Rubie

Bayerisches Geoinstitut, Universität Bayreuth, Bayreuth, Germany

Abstract. The solubility of O in Fe-rich liquid metal in equilibrium with magnesiowüstite (Mg,Fe)O was investigated at pressures to 25 GPa and temperatures to 2500°C in a 6-8 type multianvil apparatus. The experiments were designed to produce near millimetre sized pools of quenched liquid metal free of other phases, so that the equilibrium composition of the liquid metal could be recovered, taking into account the effects of quench modification. The amounts of O found in the metal are relatively small (<1 wt %) and decrease with increasing pressure at constant temperature and Mg/(Mg+Fe) ratio of the coexisting magnesiowüstite. The solubility of Si varies inversely with O and does not increase substantially with pressure when in equilibrium with mantle compositions. Experiments at 25 GPa in which silica activity is buffered by coexisting $MgSiO_3$-perovskite produce only small amounts of Si (~1 wt %) dissolved in Fe-rich metal. These results, in conjunction with cosmochemical constraints on the bulk composition of the Earth (the depletion of the Earth in cosmochemically volatile elements), leave the identity of the putative "light component" in the Earth's core as an enigma. It is difficult to account for the light component if it constitutes more than just a few percent of the core. The experiments also measure the partitioning of Fe, Ni, Co, Cr, and Ti between the Fe-rich liquid metal and magnesiowüstite phases. Ti is not significantly siderophile under the investigated conditions. When normalized to a constant metal/oxide partition coefficient for Fe, both Ni and Co become less siderophile with increasing pressure and Cr becomes more siderophile. The effect of temperature on Ni and Co partitioning is small at high temperatures, but important for Cr. The presently observed mantle abundances of Fe, Ni, Co, and Cr cannot be explained by equilibrium partitioning into the metal of the Earth's core under the pressure temperature conditions covered by the present experiments.

1. Introduction

The largest scale feature of the Earth is its differentiation into a Fe-metal rich core and a silicate mantle. Such an event is so far removed from empirical experience that it is not surprising there is little consensus as to how it happened [e.g., *Stevenson*, 1990]. There is hope, however, that some broad constraints on the physical processes may evolve from studying their chemical consequences; in particular, there are two unresolved problems regarding our understanding of the chemistry of the Earth's core-mantle differentiation, the solutions to which may illuminate our understanding of the physical processes of core formation.

The first problem is the identity of a putative "light component" in the core. Geophysical observations on the density of the Earth's core, when compared with laboratory measurements of the equation of state of iron metal extrapolated to core pressures and temperatures, indicate that the core is less dense than expected for a binary liquid Fe-Ni alloy [e.g., *Birch*, 1964; *Ahrens*, 1982]. The core is therefore thought to contain a significant amount of a light element or combination of light elements. The density deficit is currently estimated to be ~10% compared to liquid Fe-Ni, as recently reviewed by *Poirier* [1994]. Poirier quotes an uncertainty on this estimate of ± 2%. Possible elements that are (1) cosmochemically abundant enough to have an effect on core density and (2) are known to dissolve into liquid Fe-rich metal in sufficient quantities at pressure temperature conditions obtainable in the Earth, are H, C, N, O, Si, and S. All of these (except N) have had their proponents at various times; see, again, the review by *Poirier* [1994]. In an appendix to his review, Poirier estimates that the 10% density deficit requires 11 wt % S, 8.2 wt % O, or 18 wt % Si dissolved in the core. Here we present new experimental data on the solubilities of O and Si in liquid Fe at high temperatures and pressures, which show that in equilibrium with mantle material, it is unlikely that sufficient amounts of either O or Si or a combination of O and Si can dissolve into Fe-rich metal to account for a 10% density deficit. These observations, coupled with the geochemical aspects of the problem (which are somewhat complex and will be reviewed below), leave the identity of the light component as an enigma.

The second problem is "siderophile element anomaly" in the composition of the mantle. Core formation has depleted the mantle in siderophile ("metal loving") elements, but the pattern of this depletion cannot be explained satisfactorily by simple metal/silicate segregation at low pressures (*Ringwood* [1966]; see

[1] Also at Bayerisches Geoinstitut, Universität Bayreuth, Bayreuth, Germany.

[2] Now at School of Earth and Ocean Sciences, University of Victoria, Victoria, British Columbia, Canada.

Paper number 97JB02601.
0148-0227/98/97JB-02601$09.00

also recent reviews by *Palme and O'Neill* [1996] and *O'Neill and Palme* [1997]). Generally, the abundances of the moderately and highly siderophile elements are greater than predicted from low pressure metal/silicate partition coefficients, but two elements (Cr and V), which are just barely siderophile, are more depleted than would be predicted. This is the siderophile element anomaly. There are two explanations for this anomaly (not necessarily mutually exclusive): (1) the metal/silicate segregation occurred at high pressures, which may alter metal/silicate partitioning relationships sufficiently, or (2) the Earth accreted heterogeneously, with the core forming in a number of episodes of accretion and metal segregation. Heterogenous accretion/core formation implies that the present composition of the mantle is a mixture that was never in equilibrium with a single metal composition. Since Occam's razor favors the conceptually simpler equilibrium type of model, the chemical effects of core formation at high pressure need to be evaluated before the heterogenous accretion class of model is accepted. In this study we investigate the partitioning of five key elements (Fe, Ni, Co, Cr, and Ti) between liquid Fe-rich metal and magnesiowüstite solid solution to pressures corresponding to the top of the lower mantle and to near-liquidus temperatures.

2. Experimental Methodology

2.1. Experimental Strategy

There are two critical experimental problems to face in attempting to study the equilibrium between superliquidus, Fe-rich metal and possible mantle compositions at very high temperatures and high pressures. First, it is necessary to find a suitable capsule material, which ideally should contain the experimental charge without reacting chemically with it. No such material has yet been found. Here we attempt to circumvent the capsule problem by reacting the initial capsule material to one of the phases partaking in the investigated equilibrium itself; clearly, this approach is only viable if there is a solid phase which can be used as the capsule. For this reason, we have chosen magnesiowüstite, (Mg,Fe)O, both as the representative of the Earth's mantle and as the capsule material in our experiments. Magnesiowüstite is a principle phase in a mantle of peridotitic composition at depths below the 670 km seismic discontinuity and is therefore an appropriate choice for the direct investigation of mantle/metal equilibria at such pressures. At lower pressures, its use yields results that can be extrapolated to real mantle compositions with some simple thermodynamic manipulation. In this study, the high melting temperature of Mg-rich magnesiowüstite has permitted experiments up to 2500°C at 5 to 25 GPa.

The second difficulty with very high temperature, superliquidus experiments is that the high-temperature phase relations are not well preserved during quenching but need to be reconstructed from the quenched experimental run products. Problems of this kind are well known from the literature on the experimental petrology of peridotite melting, for example, the ubiquitous quench modification of picritic liquids through quench overgrowths nucleating around residual solids [e.g., *Green*, 1973]. The solution to this problem has been to try to isolate sufficiently large pools of liquid from the residual solids, for example, by conducting "sandwich" experiments [e.g., *Falloon and Green*, 1987] or, more recently, by diamond aggregate extraction techniques [e.g., *Johnson and Kushiro*, 1992]. For liquid metals, the problem is far worse even than that for picritic melts, first, because liquid metals do not form glass on quenching but crystallize completely, obscuring original textural relationships. Second, diffusion coefficients D in liquid Fe are of the order of 10^{-4} cm^2/s at ~1550°C [e.g., *Richardson*, 1974, p. 32] versus 10^{-6} to 10^{-7} cm^2/s in silicate melts at the same temperature [*Hofmann*, 1980]. The characteristic length scale over which diffusion processes operate is approximately $(Dt)^{1/2}$, and the effects of diffusion are discernible over several times this length scale. For a quench rate of 10^3 K/s from a temperature 10^3 K above the metal solidus (typical values for this study), this length scale would be ~100 μm. Thus it is necessary to isolate quenched metal pools with dimensions approaching 0.5 mm in order to characterize the composition of the original liquid metal with confidence. Indeed, migration of material over this length scale is a conspicuous feature of the run products of this study, as will be shown below. Isolating pools of quench metal of this size places severe constraints on experimental design, as current high pressure technology only permits total sample sizes of approximately this dimension.

2.2. Experimental Design

High pressure temperature experiments were performed using a 6-8 type multianvil apparatus at Bayerisches Geoinstitut, Germany. The pressure assembly consisted of Cr-doped MgO octahedra with an edge length of 18, 10, and 7 mm for experiments in the pressure ranges 3-10, 10-20, and 20-25 GPa, respectively. The furnace consisted of a cylindrical resistance heater of $LaCrO_3$. In the 18 and 10 mm sample assemblies, the temperature was measured with a W3%Re-W25%Re thermocouple inserted coaxially (with respect to the furnace), with the thermocouple junction in contact with one end of the sample capsule. In the 7 mm assembly the thermocouple was inserted radially through the furnace walls, with the junction in contact with one side of the capsule [see *McFarlane et al.*, 1994, Figure. 2]. Details of the furnace design, thermal gradients and pressure calibrations for these assemblies are given by *Rubie et al.* [1993a, b], *Canil* [1994a, b], and *McFarlane et al.* [1994]. Estimated uncertainties in pressure are of the order of ± 5%.

The samples consisted of essentially metal charges contained in capsules of MgO ceramic, machined with inner diameters of 1.0 mm for the pressure assemblies with 18 mm octahedra, and 0.5 mm for assemblies with 10 and 7 mm octahedra. Previous work showed the impurity content of the MgO ceramic to be below the routine detection limit of the electron microprobe (i.e.,< 0.1 wt % for all analyzed elements). Sample powders were packed tightly in the MgO capsules, fitted with a lid of MgO, loaded into the pressure assembly and dried overnight in vacuum at 230°C.

Five starting compositions in the system MgO-Fe-Ni-Co-Cr-Ti-(Si)-O (see Table 1) were mixed from Fe, Ni, Co, and Cr metal powders (< 50 μm) and dried SiO_2 (quartz). Ti was added as TiO_2 or as presynthesized Mg_2TiO_4 (spinel) or $MgTiO_3$ (ilmenite); MgO was either supplied from the capsule during the run or from the titanate phases. The chemicals were thoroughly mixed by grinding under acetone in an agate mortar. With the mix used in the first experiments, Si was not added intentionally, but the run products nevertheless contained Si, presumably picked up from the agate mortar. Experiments using mixtures with added SiO_2 resulted in run products with Si contents in the metal identical to those in the nominally Si-free experiments run at the same pressure temperature conditions (Table 1), showing that sufficient Si had been picked up to saturate the latter.

For each experiment, the sample was pressurized at room temperature to the run pressure and then heated to the desired

Table 1. Experimental Runs

Run	Starting Mix	P, GPa	T, °C	Time, mins	Blobs, vol %	Comments
UHP1027	a	5	1800	30	0.18(0.09)	very small blobs, <1 μm
UHP986	a	5	2200	10	2.9(0.5)	
UHP981	a	9	2200	30	3.7(1.3)	
UHP1036	a	9	2200	11.5	0	"slowly" quenched (600°C/min); no blobs
UHP1069	b	9	2200	15	5(1.3)	Ti added as Mg_2TiO_4
UHP1180	c	9	2200	16	4.6(0.5)	
UHP1183	d	9	2200	16	3.3(0.4)	
UHP984	a	9	2400	2	3.4(0.5)	
H111	a	18	2200	3	1.0(0.3)	
H143	a	21	2200	4	1.4(0.2)	
UHP1081	e	25	2500?	4	?	+ perovskite; sample mostly lost in preparation
UHP1087	e	25	2500	15	2.0(0.5)	+ perovskite

P is pressure; T is temperature. Starting mixes are as follows: a, 78 % Fe, 16.9% Ni, 1.3% Co,1.7%Cr, 2.1%TiO_2; b, same as a, but Ti added as Mg_2TiO_4; c, same as a, plus 5% SiO_2; d, same as a, plus 10% SiO_2; and e, same as a, plus 15% SiO_2, and Ti added as $MgTiO_3$. Numbers in parentheses are standard deviations.

temperature at a rate of 100°C/s to 200°C/s. With the exception of run UHP1036, which was cooled at a controlled rate, runs were quenched by cutting power to the furnace. Quench rates of the order of 1000°C/s to 2000°C/s are achieved with this method because of the small dimension and low thermal mass of the the resistance heaters. After quenching, samples were decompressed over a period of 12 to 24 hours. The entire sample plus pressure assembly was then mounted in epoxy, sectioned approximately through its center, and polished for examination by reflected light microscopy, backscattered electron imaging, and subsequent electron microprobe analysis.

2.3. Experimental Run Products

At the start of an experiment, the charge is composed of the starting mixture of metal plus minor oxide components packed inside a pure MgO capsule. At the completion of the experiment, the recovered quenched run products consisted of four or five separately identifiable components: (1) a diffusion profile of FeO plus oxides of Ni, Co, Cr, Ti and some Si extending from the original metal/MgO interface into the MgO capsule (thus the original MgO capsule is converted to (Mg,Fe)O solid solution where it is in contact with the metal); (2) inside the original MgO

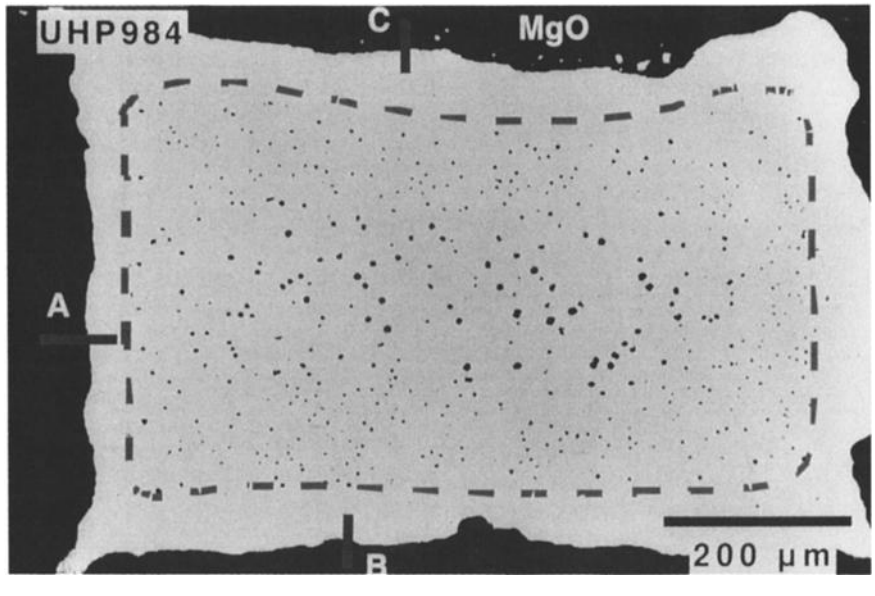

Figure 1a. Backscattered electron images of experimental run product. UHP984 (2400°C, 9 GPa). Dark gray blobs of Si-O-Cr-rich material (produced on the quench) in a light gray Fe-Ni metal matrix. The MgO capsule is black. The blobs are conspicuously absent from a zone of ~100 μ bordering the MgO capsule; marked by a dashed curve. The Si-Cr-O material from the blob free border zone occurs along the metal/MgO contact, although this cannot be seen in the images. Analytical profiles were taken normal to the interface between the Mg capsule and the metal at points labelled A, B and C. The results for profile A are displayed in Figure 2. This particular run shows a marked gradient in the size of the blobs from the middle outward, which is not as well developed or is entirely absent in other runs.

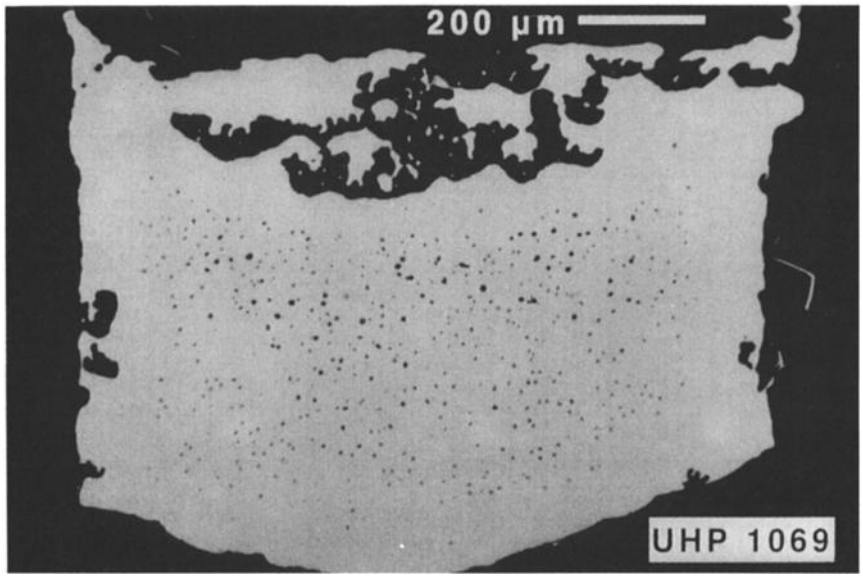

Figure 1b. Backscattered electron images of experimental run product. UHP1069 (2200°C, 9 GPa). The quench blobs are not preserved in the "islands" of metal at the top. We suggest that satisfactory quenching of O-containing liquid metals demands metal pools greater than several hundred micrometers in size, even for multianvil quench rates.

capsule, solid Fe-Ni-Co-Cr metal also containing some Si (hereafter referred to as "matrix metal"); (3) semispherical blobs of O-Si-Cr-rich material dispersed in the matrix metal, except within about 100 μm of its margins with the (Mg,Fe)O capsule; (4) a smear of O-Si-Cr material along the interface between the matrix metal and the (Mg,Fe)O capsule; and (5) for the two experiments at 25 GPa (UHP1081 and UHP1087), anhedral crystals of $MgSiO_3$-perovskite inside the MgO capsule; with dimensions up to 50 μm.

Backscattered electron images of two typical run products and a closeup of blobs from a third run are shown in Figures 1a-1c. Extending from the original interface between the MgO capsule and the Fe-rich metal charge, a diffusion profile of FeO plus other elements from the charge (Cr, Ti, Ni, and Co; all presumably as oxides) runs into the MgO, typically traceable for > 200 μm (e.g., Figure 2). The extent of the diffusion profile can easily be seen in the polished sections in reflected light using oblique illumination. Inside the MgO capsule, what we interpret (see below) single phase, liquid Fe-rich metal at the tempreature and pressure of the run, has quenched to a curious texture of rounded, sometimes discernibly hexagonoid "blobs," usually 1 to 20 μm in diameter, set in a matrix of solid Fe-rich metal (the hexagonal shape of the blobs is much more clearly developed in some runs than others, for unknown reasons). Compositions of both blobs

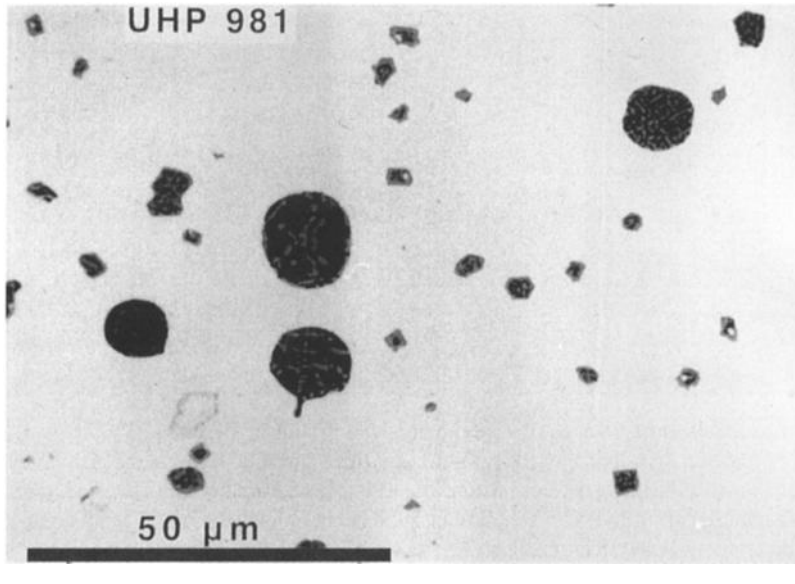

Figure 1c. Close-up of quench blobs in UHP981 (2200°C, 9 GPa), showing them to be a mixture of at least two phases.

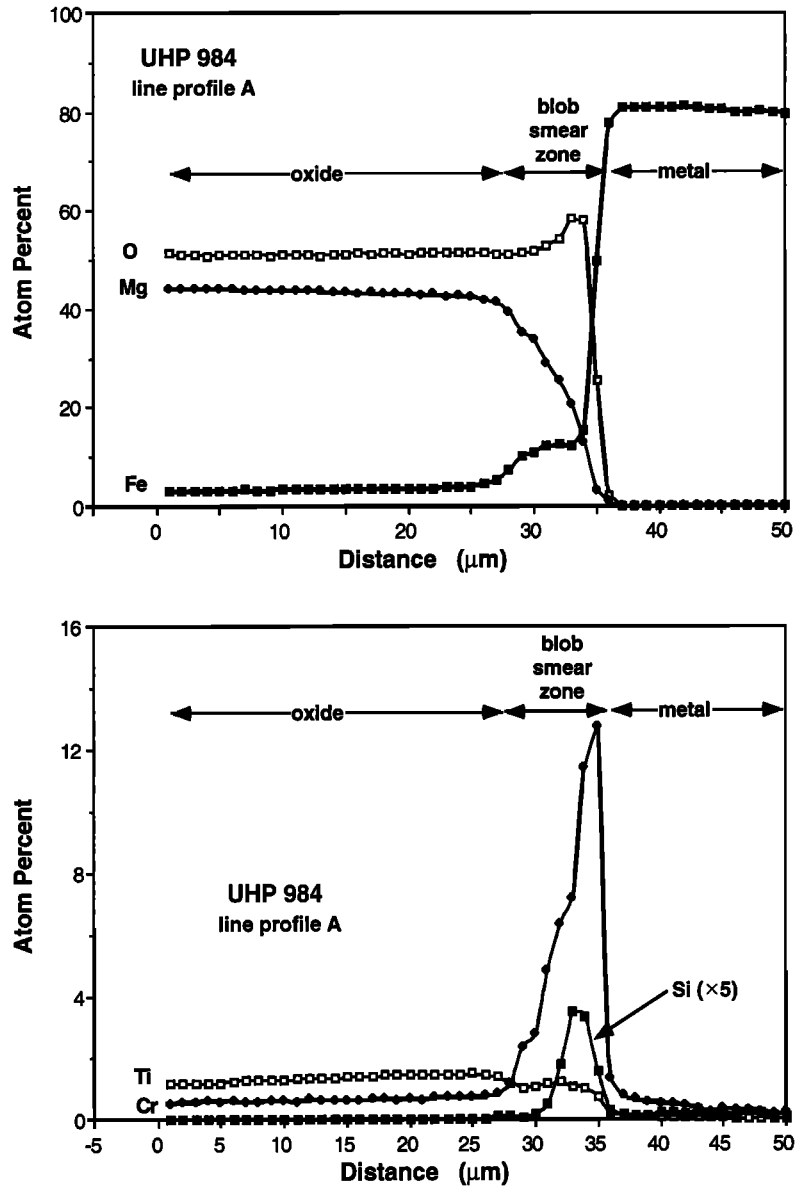

Figure 2. Electron microprobe profile analyses across section A of Figure 1a. During the run, FeO plus minor constituents (NiO, CoO, Cr_2O_3, TiO_2) diffuse from the metal/oxide starting material into the MgO capsule for distances up to ~100 μm. The blob smear zone at the contact between the magnesiowüstite and the matrix metal is composed of the same constituents (Si, O, and Cr) as the exsolution blobs in the interior of the matrix metal and is presumed to be caused by the heterogenous nucleation and diffusion of this component of the liquid metal during quenching.

and matrix metal are given in Table 3. The blobs, which themselves are a fine grained (submicron scale) intergrowth of at least two, perhaps more, phases (unidentified, but reasonably presumed to be mostly chromite plus one or more Fe-silicate phases at ≤ 9 GPa and stishovite plus an $FeO\text{-}SiO_2$ silicate phase at 25 GPa), carry all of the O, nearly all the Ti, and a substantial fraction of the Si and Cr contents of the original liquid metal. They do not contain any measurable Mg (an indicator to their secondary origin). Similar blobs were described *by Ohtani and Ringwood* [1984], *Kato and Ringwood* [1989], *Ringwood and Hibberson* [1990, 1991], and, recently, by *Ito et al.* [1995]. Intriguingly, very similar blobs have also been described in the Fe-rich metal of some unequilibrated chondrites [*Zanda et al.*, 1994].

As is evident from Figure 1, the blobs are absent from the region bordering the MgO capsule (as also found by *Ohtani and Ringwood* [1984]. This feature is conspicuously present in all runs produced by the normal poweroff quenching method, and we believe that it is of considerable significance. The blob free border zone parallels the capsule/metal interface, and where "xenoliths" of MgO have become detached from the capsule and separated into the metal (Figure 1b), the blob free border zone also follows that the outline of the xenolith. It appears that in this border region, the O-Si-Cr-rich material which elsewhere forms the blobs has migrated to the capsule/metal interface during the quench. Although this is not evident from either reflected light microscopy or backscattered electron imaging, the existence of a smear of blob material along the interface becomes readily

apparent when an analytical profile is made across the interface (Figure 2). This phenomenon suggests that blob formation is controlled by the kinetics of homogenous nucleation. The blob free border zone is formed because the O-Si-Cr-rich material can nucleate heterogeneously along the capsule wall and migrate through the matrix metal over ~100 μm in the timescale over which the blobs form, because of the high rates of diffusion in liquid Fe.

That the blobs are quench features and not a primary, coexisting immiscible liquid is indicated first by their chemistry. As pointed out above, they contain virtually no MgO (Table 3). This is true even when MgO is present in the starting material, as Mg_2TiO_4 or $MgTiO_3$. For example, run UHP1069 (with TiO_2 added as Mg_2TiO_4) contains blobs having similar Ti and similarly negligible Mg as the runs using the MgO-free starting material. Run UHP1069 is thus a reversal experiment confirming that the negligible Mg content of the blobs is an equilibrium phenomenon. The MgO in the starting material cannot be found within the capsule and presumably has migrated to the capsule wall. If the blobs represent a primary silica-containing oxide melt, then, since this melt would have been in equilibrium with high Mg magnesiowüstite, it would be expected to contain a substantial amount of MgO.

Second, we performed a run that was terminated not by the usual poweroff quench but rather, by controlled cooling to room temperature at a rate of 600°C/min (UHP1036, identical P-T conditions to UHP981, UHP1180, and UHP1183). The run product was entirely blob free, but the O-Si-Cr-rich component could still be found at the capsule/metal interface. The comparatively "slow" cooling rate appears to have extended the blob free border zone to encompass the entire charge. This is reasonable, considering the characteristic diffusion rates in liquid Fe ($D \sim 10^{-4}$ cm^2/s at 1550°C).

2.4. Electron Microprobe Analysis

A preliminary examination of the run products was made using the CAMECA SX50 electron microprobe at the Bayerisches Geoinstitut, Universität Bayreuth. Quantitative electron microprobe analyses were then performed at the Research School of Earth Sciences, The Australian National University, on the CAMECA Camebax, using the following analytical procedures.

1. Matrix metal was analyzed for Fe, Ni, Co, Cr, Ti, and Si, and the magnesiowüstite adjacent to the metal was analyzed for MgO, FeO, NiO, Cr_2O_3, TiO_2, and SiO_2 (oxygen by stoichiometry) by energy dispersive spectrometry (EDS) using a Si(Li) detector (see *Ware* [1991] for further instrumental details). Operating conditions were an accelerating voltage of 15 kV; a beam current of ~2.2 nA; counting time 80 s (corrected for dead time); with standardization on pure Fe, Co, and Ni metals, $CaSiO_3$ (wollastonite) for Si, TiO_2 (rutile) for Ti, Cr_2O_3 for Cr (checked on Cr metal), and MgO for Mg. This procedure is not optimal for Co owing to overlap from the Fe peak; therefore for Co, we preferred results from wavelength-dispersive spectrometry (WDS).

2. Ni and Co were analyzed in the magnesiowüstite and, in UHP1087, in the coexisting $MgSiO_3$-rich perovskite using WDS, and an accelerating voltage of 25 kV with a 35 nA beam current, thallium hydrogen phthalate (TAP) crystals for Mg and Si, pentaerythritol (PET) for Cr and Ti, and LiF for Fe, Co, and Ni. Counting times were 60 s on background and peaks, except for Fe, which was 40 s. Checks on San Carlos olivine (2900 ppm Ni) were made from time to time (see *Ware* [1991]). This routine was also used to check the composition of the matrix metal from the EDS analyses; agreement was found to be complete, except for Co, for which minor differences (<0.3 wt %) probably reflect the severe overlap problem with Fe in the energy-dispersive spectrum.

3. The blobs were analyzed for oxygen together with the other major elements, using WDS. A WSi crystal was used for O. Conditions were 15 kV and 40 nA, with standards as above, plus MgO for O. Counting times were 160 s for O, 80 s for Si and Mg, and 40 s for Ti, Cr, Ni, and Fe. The shape of the background for O was empirically established by assuming zero O in the solid Fe metal standard.

Generally, except for the blob analyses in runs with large blobs, the electron beam diameter was ~2 μm, which is the standard focused beam size for this instrument. For analysing the larger blobs, the beam was defocused up to a diameter of ~10 μm, so as to obtain an average composition of the blob from its intergrown phases.

3. Experimental Results

3.1. Composition of the Magnesiowüstite at the Metal/Oxide Interface

We assume that the composition of magnesiowüstite in chemical equilibrium with the liquid metal is that at the interface with the metal. This assumption of local equilibrium is reasonable as diffusion rates in the liquid metal are $>10^4$ faster than those of Fe in magnesiowüstite (magnesiowüstite diffusion data are summarized by *Freer* [1980]). This interface composition was obtained as follows. A series of point analyses was made along a line perpendicular to the interface, at 1 to 3 μm intervals, extending from 20 to 100 μm into the oxide, across the interface (including the smear of O-Si-Cr-rich material), and into the matrix metal. Plots were then made of the concentration of the analyzed elements versus distance from the interface. For the trace elements Co and Ni, it was necessary sometimes to eliminate a few anomalously high analyses, especially near the interface. This is justified because the roughness of the interface extends into three dimensions, whereas seemingly suitable sites for the diffusion profile must be chosen from the two-dimensional polished surface, and any overlap with unseen metal will grossly distort the analysis. Nevertheless, selecting data necessarily introduces some element of subjectivity, and for this reason, we give the uncertainty for the Ni and Co contents of the magnesiowüstite as 5% plus 50 ppm, 1 standard deviation. The element concentration profiles are, as expected from theoretical considerations [e.g., *Darken and Gurry*, 1953, p. 443], effectively linear in the vicinity near the interface (see, e.g., Figure 2). In order to obtain the best estimate of the value at the interface, the concentrations were linearly regressed against distance from the interface, and the regression value at the interface was selected. Four to seven such profiles were made using the EDS routine, and two profiles for Ni and Co were made using the WDS routine. In addition, several spot analyses at suitable points in the magnesiowüstite within 20 μm of the interface were obtained with both analytical routines. These were used, together with the regression values, to obtain the mean and standard deviation of values of the composition of the magnesiowüstite at the interface, reported in Table 2.

Table 2. Analyses of Magnesiowüstite Solid Solutions Near Oxide/metal Interface

	UHP1027	UHP986	UHP981	UHP1036	UHP1069	UHP1180	UHP1183	UHP984	H111	H143	UHP1081	UHP1087
P, GPa	5	5	9	9	9	9	9	9	18	21	25	25
T, °C	1800	2200	2200	2200	2200	2200	2200	2400	2200	2200	2500?	2500
SiO_2	0.24(0.09)	0.04(0.01)	<0.10	0.27(0.07)	<0.10	<0.10	0.11(0.10)	<0.10	0.10(0.10)	<0.10	0.16(0.10)	<0.10
TiO_2	4.63(1.31)	1.74(0.10)	3.27(0.19)	3.12(0.21)	3.15(0.38)	0.97(0.03)	0.76(0.08)	5.92(0.85)	3.94(0.24)	3.13(0.20)	0.61(0.16)	0.75(0.06)
Cr_2O_3	3.99(0.13)	3.02(0.05)	2.60(0.23)	5.24(0.68)	3.14(0.07)	2.38(0.06)	2.46(0.15)	2.30(0.20)	1.62(0.04)	1.63(0.16)	1.45(0.31)	1.68(0.05)
FeO	9.88(0.17)	11.45(0.30)	12.92(1.04)	14.31(0.63)	13.78(0.42)	15.65(0.47)	15.33(0.32)	12.54(0.94)	11.72(0.60)	14.55(0.63)	12.95(0.39)	13.59(0.38)
NiO	0.11(0.07)	0.20(0.12)	0.22(0.08)	0.20(0.07)	0.23(0.05)	0.28(0.06)	0.30(0.05)	0.25(0.11)	0.34(0.09)	0.49(0.10)	0.62(0.12)	0.71(0.07)
MgO	81.15(1.57)	83.55(0.38)	80.89(1.10)	76.87(1.45)	79.60(0.42)	80.64(0.56)	81.03(0.49)	78.99(1.74)	82.27(0.72)	80.19(0.73)	84.22(0.71)	83.17(0.41)
Co, ppm	270	350	550	n.a.	480	600	610	470	520	650		810
Ni, ppm	1300	1420	2220	n.a.	2290	2780	2720	1990	3000	4020		5470
Cations												
Si	0.0018(7)	0.0003(1)	0	0.0020(6)	0	0	0.0008(7)	0	0.0007(7)	0	0.0012(7)	0
Ti	0.0255(72)	0.0095(5)	0.0181(11)	0.0176(12)	0.0175(21)	0.0053(2)	0.0042(4)	0.0331(47)	0.0216(13)	0.0173(11)	0.0033(9)	0.0041(3)
Cr	0.0232(7)	0.0397(3)	0.0151(13)	0.0310(40)	0.0184(4)	0.0138(4)	0.0143(9)	0.0135(12)	0.0093(2)	0.0095(9)	0.0082(18)	0.0097(3)
Fe	0.0606(11)	0.0694(18)	0.0794(64)	0.0897(39)	0.0852(26)	0.0961(29)	0.0939(20)	0.0719(58)	0.0715(40)	0.0896(39)	0.0781(23)	0.0824(23)
Mg	0.888(17)	0.902(4)	0.885(12)	0.858(16)	0.877(5)	0.883(6)	0.885(5)	0.874(19)	0.895(8)	0.881(8)	0.906(8)	0.899(4)

The uncertainty in the trace element analyses for Co and Ni are taken to be (50 ppm + 5%). Numbers in parentheses are standard deviations. Here n.a. means not analyzed.

3.2. Compositions of the Matrix Metal

The composition of the matrix metal was found to be nearly homogenous in all runs. Mean compositions with standard deviations from at least 10 EDS analyses and five WDS analyses for Fe, Ni, Cr, Ti, and Si are given in Table 3. For Co, the WDS analyses are expected to be considerably more accurate than the EDS analyses and were indeed found to give more precise results (lower standard deviations). Hence for Co, only WDS analyses are reported.

The matrix metal contained negligible Ti, except for run UHP 984. Mg was included in the analytical routine in both the WDS and EDS analyses but was below the detection limit (0.03 wt % for WDS analyses) in all runs.

3.3. Compositions of the Blobs

The blobs posed a special analytical problem, in that they consisted of intergrowths of two or more phases, each with dimensions too small to be determined individually but often large enough to prevent the focused electron beam (~2 μm) from obtaining a reasonable average. Mean blob compositions were determined in two ways.

1. For runs containing sufficient blobs of a size larger than ~5 μm, the beam was defocused to a diameter just smaller than that of the blob, so as to obtain an average analysis of nearly all the exposed section of the blob. For those runs with fine grained intergrowths of coexisting quench phases in their blobs, replicate analyses with this procedure gave results with quite small standard deviations (e.g., UHP1180). For runs in which the quench phases in the blobs were of a size comparable to the blobs themselves, the standard deviations are, of course, larger (e.g., UHP1069). This probably does not reflect bulk heterogeneity between blobs but, rather, the difficulty of obtaining a representative composition in a single analysis.

For each of these runs, the valence state of Cr in the blobs was computed, assuming a valence state of 2+ for Fe and Ni and 4+ for Ti and Si. The results, which also serve as a monitor of the accuracy of the O analyses, are given in Table 3. In nearly every case, the Cr is within experimental error of a valence state of 3+ (anything between 2+ and 3+ might have been expected *a priori*).

2. For runs with blobs <5 μm (UHP1027, H111, H143, and UHP1087), even using a focused beam gives mixed analyses of blob plus matrix metal. Blob compositions were extracted from these mixed analyses by mass balance; for each individual analysis, the composition of the matrix metal was subtracted to the point at which the O becomes sufficient to balance the remaining Fe, Ni, Cr, Ti, and Si in their appropriate valence state using a valence of 3+ for Cr, as deduced from the larger blobs. A further check on the efficacy of this procedure is that the calculated Ni in the blobs should be small, but not negative. The few calculated compositions that had unrealistic Ni-contents were discarded, and the rest were averaged (Table 3).

3.4. Reintegrated Liquid Metal Compositions

The composition of the original single phase liquid metal may be estimated from the compositions of the blobs and the matrix metal if their relative proportions are known. Six representative rectangular areas were selected from the middle of each charge (i.e., away from the blob free border zones), and backscattered electron images were obtained. These images were analyzed using ImageWriter software to determine area, hence volume, of

Table 3. Metal Analyses

Run	UHP1027	UHP986	UHP981	UHP1036	UHP1069	UHP1180	UHP1183	UHP984	H111	H143	UHP1081	UHP1087
						Matrix						
Si	0.00	0.07(0.07)	0	0	0.10(0.05)	0.18(0.04)	0.29(0.18)	0.01(0.01)	0.14(0.01)	0.06(0.05)	1.21(0.11)	0.93(0.07)
Ti	0.00	0	0	0	0	0	0	0.04(0.01)	0	0	0.01(0.02)	0
Cr	0.39(0.03)	0.46(0.02)	0.30(0.07)	0.89(0.38)	0.33(0.12)	0.16(0.12)	0.11(0.02)	0.32(0.02)	0.64(0.17)	0.39(0.11)	0.85(0.09)	0.96(0.05)
Fe	80.54(0.51)	80.46(0.59)	79.41(0.37)	79.01(0.61)	79.52(0.62)	78.41(0.52)	77.89(0.60)	80.41(0.36)	79.95(0.60)	80.36(0.27)	77.54(0.99)	77.79(0.33)
Co	1.44(0.03)	1.20(0.13)	1.78(0.14)	1.44(0.09)	1.27(0.11)	1.50(0.09)	1.52(0.11)	1.46(0.04)	1.47(0.04)	1.26(0.08)	0.98(0.08)	1.33(0.10)
Ni	17.63(0.39)	17.80(0.21)	18.49(0.32)	18.66(0.37)	18.78(0.76)	19.75(0.62)	20.19(0.32)	17.77(0.35)	17.80(0.21)	17.94(0.47)	19.42(0.66)	18.99(0.14)
						Blobs						
wt %	0.11(0.06)	1.8(0.3)	2.3(0.8)	0, all in rim	3.2(0.8)	2.9(0.3)	2.1(0.3)	2.2(0.3)	0.6(0.2)	0.9(0.1)	n.d.	1.3(0.5)
Si	3.26(2.13)	10.53(2.01)	9.00(1.7)		9.05(3.27)	4.84(0.36)	7.24(0.96)	2.93(0.50)	9.17(1.93)	9.16(0.90)		36.70(1.54)
Ti	0.33(0.25)	0.42(0.24)	1.24(0.56)		0.82(0.49)	0.13(0.02)	0.10(0.03)	0.24(0.09)	3.20(2.55)	3.04(1.68)		0.12(0.03)
Cr	28.28(6.77)	27.52(4.33)	20.08(4.87)		17.37(7.70)	16.93(1.43)	17.20(3.87)	25.92(0.96)	10.76(1.89)	12.98(1.51)		0.38(0.05)
Fe	39.24(3.55)	27.09(1.59)	36.99(2.12)		41.28(2.25)	49.91(2.78)	45.33(2.64)	43.05(1.60)	46.74(9.64)	44.19(4.80)		15.49(3.27)
Ni	0.56(1.02)	0.29(0.14)	0.37(0.18)		0.67(0.39)	0.25(0.14)	0.43(0.35)	1.42(0.72)	(0)	0.17(0.43)		0.51(1.23)
Mg	0.02(0.02)	0.19(0.22)	0.12(0.04)		0.14(0.11)	0.06(0.04)	0.03(0.01)	0.06(0.08)	0.04(0.02)	0.03(0.02)		0.09(0.03)
O	28.41(0.19)	33.96(0.46)	32.20(0.51)		30.67(0.63)	27.88(0.41)	29.67(0.31)	26.38(0.47)	29.96(0.76)	30.53(1.74)		46.71(0.45)
Cr valence	n.d.	3.2(0.2)	2.2(1.7)		2.9(0.4)	3.0(0.2)	3.1 (0.2)	2.5(0.1)	n.d.	n.d.		n.d.
						Integrated Metal						
Si	<0.01	0.25(0.08)	0.21(0.08)		0.39(0.14)	0.32(0.04)	0.44(0.18)	0.07(0.02)	0.19(0.02)	0.14(0.05)		1.40(0.20)
Cr	0.42(0.04)	0.95(0.11)	0.75(0.21)		0.88(0.31)	0.65(0.13)	0.47(0.10)	0.88(0.08)	0.70(0.17)	0.50(0.11)		0.95(0.33)
Fe	80.49(0.51)	79.50(0.63)	78.43(0.79)		78.30(0.94)	77.58(0.58)	77.21(0.65)	79.59(0.45)	79.75(0.63)	80.03(0.29)		76.87(0.41)
Co	1.44(0.03)	1.18(0.13)	1.74(0.14)		1.22(0.11)	1.46(0.09)	1.49(0.11)	1.43(0.04)	1.46(0.04)	1.25(0.08)		1.31(0.14)
Ni	17.61(0.39)	17.48(0.21)	18.07(0.35)		18.20(0.75)	19.18(0.60)	19.78(0.32)	17.41(0.35)	17.69(0.21)	17.78(0.47)		18.75(0.10)
O	0.03(0.02)	0.61(0.10)	0.74(0.26)		0.98(0.25)	0.81(0.08)	0.62(0.09)	0.58(0.08)	0.18(0.06)	0.27(0.03)		0.61(0.23)
D_{Cr}	0.154(0.014)	0.46(0.06)	0.42(0.12)		0.41(0.14)	0.40(0.08)	0.29(0.06)	0.56(0.06)	0.63(0.16)	0.45(0.11)		0.83(0.30)
D_{Fe}	10.5(0.2)	8.9(0.2)	7.8(0.63)		7.3(0.2)	6.4(0.2)	6.5(0.1)	8.2(0.2)	8.75(0.25)	7.1(0.2)		7.3(0.2)
D_{Co}	53(13)	34(7)	32(5)		26(5)	24(4)	24(4)	30(5)	28(4)	19(3)		16(2)
D_{Ni}	135(12)	123(11)	81(6)		79(7)	69(5)	73(5)	87(7)	59(4)	44(3)		34(2)

Numbers in parentheses are standard deviations. Here n.d. denotes not determined. *D* is distribution coeffiicient.

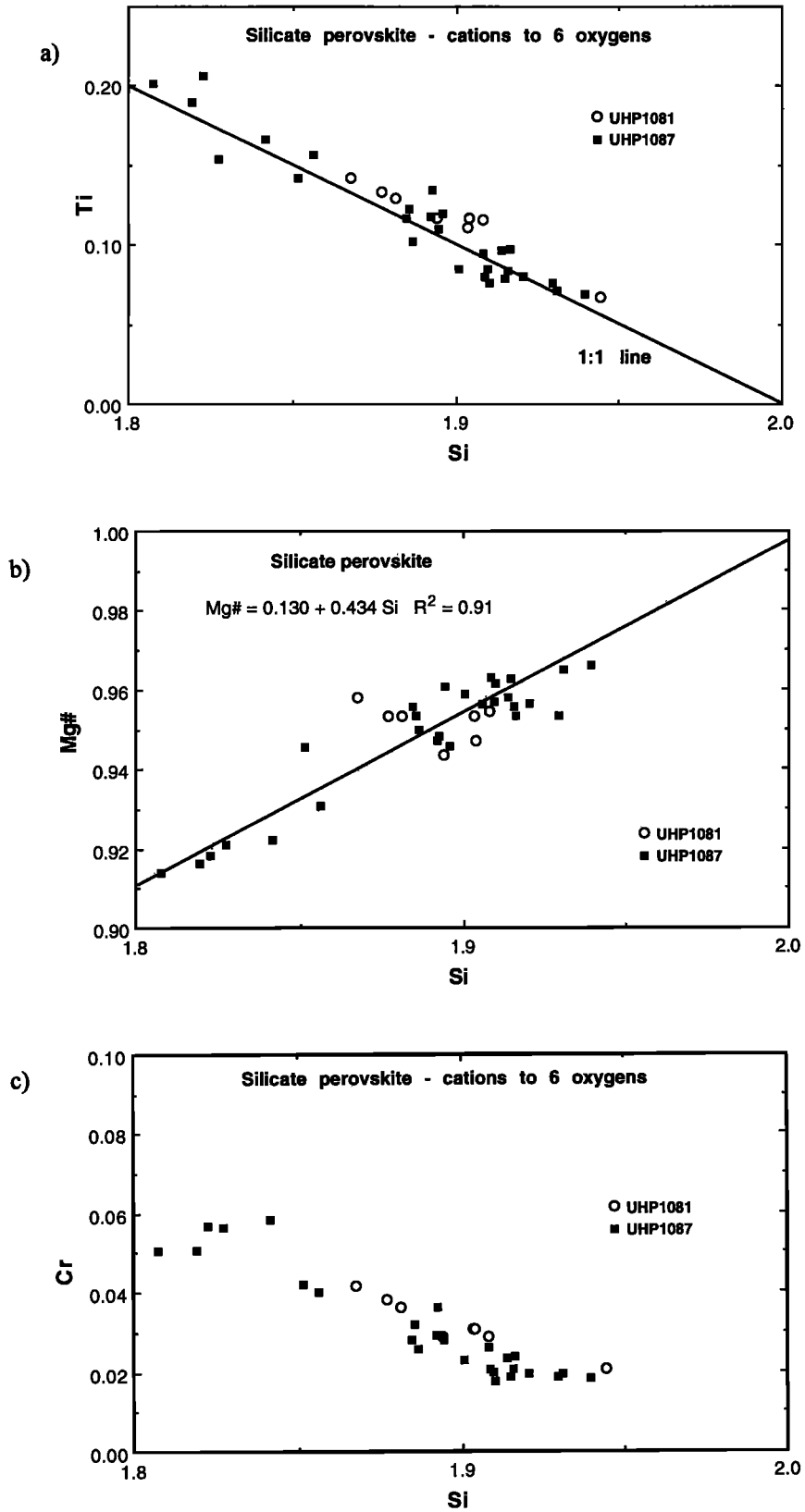

Figure 3. Perovskite chemistry in runs UHP1081 and UHP1087. (a) Negative correlation of Ti and Si. The proximity of the correlation with the 1:1 slope argues for the substitution of Ti for Si as homovalent, i.e., Ti^{4+} for Si^{4+}. (b) Correlation of Mg # (Mg/(Mg+Fe) with Si, hence also with Ti. (c)A rather less pronounced correlation of Cr with Si, hence also with Ti and Mg #.

blob material. Means and standard deviations of the volume percentage of blobs are given in Table 1. These volume percentages were converted to weight percentages (given in Table 3) assuming a density of the blob material of 4.5 g/cm^3 (appropriate for Fe_2SiO_4 spinel, $FeCr_2O_4$, and SiO_2 stishovite, which are probably the main constituents of most of the blobs) and a density of 8 g/cm^3 for matrix metal.

3.5. Silicate Perovskite Chemistry

The two runs at 25 GPa and ~2500°C crystallized $MgSiO_3$-rich perovskite, which occurs within the metal part of the charge as anhedral crystals with grain sizes up to 50 μm. This relatively large grain size (for experimentally produced silicate perovskites) allows good quality electron microprobe analysis, and therefore as the perovskite coexists with the magnesiowüstite of the capsule, it allows for the determination of the partitioning relations of Fe, Co, and Ni between the two major phases of the lower mantle. The perovskite does damage very easily under the electron beam, however. Electron microprobe analyses were made using EDS and relatively short counting times for Mg, Si, Fe, Ti, and Cr in both runs, with additional analyses for Co and Ni undertaken on UHP1087 with WDS using the longer counting times.

The perovskites in both runs have variable compositions owing to substitution of Ti for Si (Figure 3a). The extent of this substitution ranges from 3 to 10% on an atomic basis and appears, at least in UHP1087, to show some systematic spatial correlation; perovskite grains near the middle of the capsule, adjacent to the thermocouple and therefore presumably near the hottest part of the assembly, have higher Ti contents. This kind of correlation with temperature would be expected if the solubility of Ti in the perovskite is controlled by a solvus or miscibility gap, for example, between the $MgSiO_3$-rich perovskite phase and a $MgTiO_3$-rich phase, perhaps of a different structure (e.g., ilmenite), although no such phase was found.

The perovskites show a remarkably strong correlation of Fe with Ti (Figure 3b). A similar correlation of Fe with Al was recently shown in experiments by *Wood and Rubie* [1996], presumably due to the coupled substitution of Fe^{3+} with Al. The presence of enhanced levels of Fe^{3+} in Al-containing perovskites has been confirmed by *McCammon* [1997], using Mössbauer spectroscopy. Here, however, a coupled-charge-balanced substitution involving Fe^{3+} and Ti^{3+} is unlikely on several grounds. First, the presence of Ti^{3+}, an oxidation state of Ti that usually occurs under highly reducing conditions, is empirically found to be incompatible with Fe^{3+}, at least in low pressure silicate minerals. Second, the variation of Ti with Fe is not in the 1:1 ratio predicted by the coupled substitution relationship (see Figure 3a and 3b). Rather, the relationship shown in Figure 3a strongly suggests the substitution of Ti^{4+} for Si^{4+}. The phenomenon may therefore indicate a strong reciprocal solid solution effect [*Wood and Nicholls*, 1978], with a large positive Gibbs free energy for the reciprocal reaction:

$$\underset{\text{pvsk}}{MgSiO_3} + \underset{\text{pvsk}}{FeTiO_3} = \underset{\text{pvsk}}{FeSiO_3} + \underset{\text{pvsk}}{MgTiO_3} \quad (1)$$

Where pvsk is perovskite. As a further complication, Fe is also correlated with Cr (see below), which could perhaps be explained by a charge coupled substitution. A detailed investigation of Cr- and Ti-rich perovskites by Mössbauer spectroscopy would be needed to resolve this problem.

Empirical linear extrapolation of the trend in Figure 3b implies an Mg # of > 0.99 for pure silicate (Ti- free) perovskite and hence the distribution coefficiency $KD^{ox/pvsk}_{Mg\text{-}Fe} < 0.1$. This result is in reasonable agreement with the Fe-Mg partitioning studies of *Ito et al.* [1984] and *Fei et al.* [1991] in the simple system MgO-SiO_2-Fe-O. They obtained mean values for the empirical $KD^{ox/pvsk}_{Mg\text{-}Fe}$ of ~0.15 and 0.13±0.01 at 26 GPa and 1600°C and 1400°C, respectively. Our results are also in agreement with the studies of *Ohtani et al.* [1991] (at 27 GPa/1700°C and 25 GPa/1900°C) and *Kesson and Fitz Gerald* [1991] in a diamond anvil cell, who also investigated systems without Al or Ti. Much higher values of $KD^{ox/pvsk}_{Mg\text{-}Fe}$, up to and even slightly greater than unity, have been observed in other work in which the perovskite is aluminous [e.g., *Irifune*, 1994; *McFarlane et al.*, 1994; *Wood and Rubie*, 1996]. Here the most Ti-rich perovskites also define $KD^{ox/pvsk}_{Mg\text{-}Fe} \approx 1$.

Cr in the perovskite is also positively correlated with Ti (hence with Fe), reaching nearly 2 wt % Cr_2O_3 at 0.2 atoms Ti per formula unit and extrapolating to approximately zero at the silicate end member (Figure 3c). Cr_2O_3 in the coexisting magnesiowüstite is ~1.6 wt %. The distribution of Cr between perovskite and magnesiowüstite in natural compositions is thus also likely to depend on the details of the perovskite chemistry.

The Ni and Co abundances in the perovskites do not show a correlation with the Si/Ti ratio within the precision of the data (Figure 4). The mean values of these abundances, when combined with the Ni and Co contents of the coexisting magnesiowüstite at the metal/magnesiowüstite interface (Table 2), give values of empirical Nernst partition coefficients $D^{ox/pvsk}_{Ni} = 5.2$ and $D^{ox/pvsk}_{Co} = 4.2$. The strong preference of Ni for magnesiowüstite over coexisting perovskite is in agreement with previous findings [*Kesson and Fitz Gerald*, 1991; *Ohtani et al.*, 1991; *McFarlane et al.*, 1994; *Malavergne et al.*, 1997]. The magnitude of $D^{ox/pvsk}_{Ni}$ found here is in fairly good agreement with the values found in the first three of these studies, but is somewhat less than that found by *Malavergne et al.* [1997], who obtained $D^{ox/pvsk}_{Ni} > 33$ at 1500 to 3000 K and 26 to 70 GPa. However, the value of $D^{ox/pvsk}_{Co}$ found here is in very good agreement with that obtained by *Malavergne et al.* [1997], and also with that of the only other previous study, *Ohtani et al.* [1991]. Making the reasonable assumption that all the lower mantle's Ni and Co reside in its Ni-Co-rich magnesiowüstite or its modally dominant $MgSiO_3$-rich perovskite allows bulk-mantle/metal partitioning coefficients for Ni and Co to be calculated, through which the effects of core formation on the mantle's abundance of Ni and Co may be quantitatively modeled.

4. Discussion

4.1. Fe-Co-Ni Partitioning Between Magnesiowüstite and Liquid Fe-rich Metal

From the compositions of the oxide at the metal/oxide interface (Table 2) and the reintegrated liquid metal compositions (Table 3), we can compute metal/oxide distribution coefficients, $D^{met/ox}_M$. (Distribution coefficients can be defined either by weight concentrations or mole fractions; here we choose the latter for ease of comparison with thermodynamic calculations.)

In their raw form, such empirical distribution coefficients have limited usefulness, since the distribution of a siderophile element between metal and oxide (or silicate) depends strongly on oxygen fugacity, a quantity not measured directly in the experiments. This is easily appreciated if the partitioning equilibrium is written out explicitly as a mass-balanced chemical reaction:

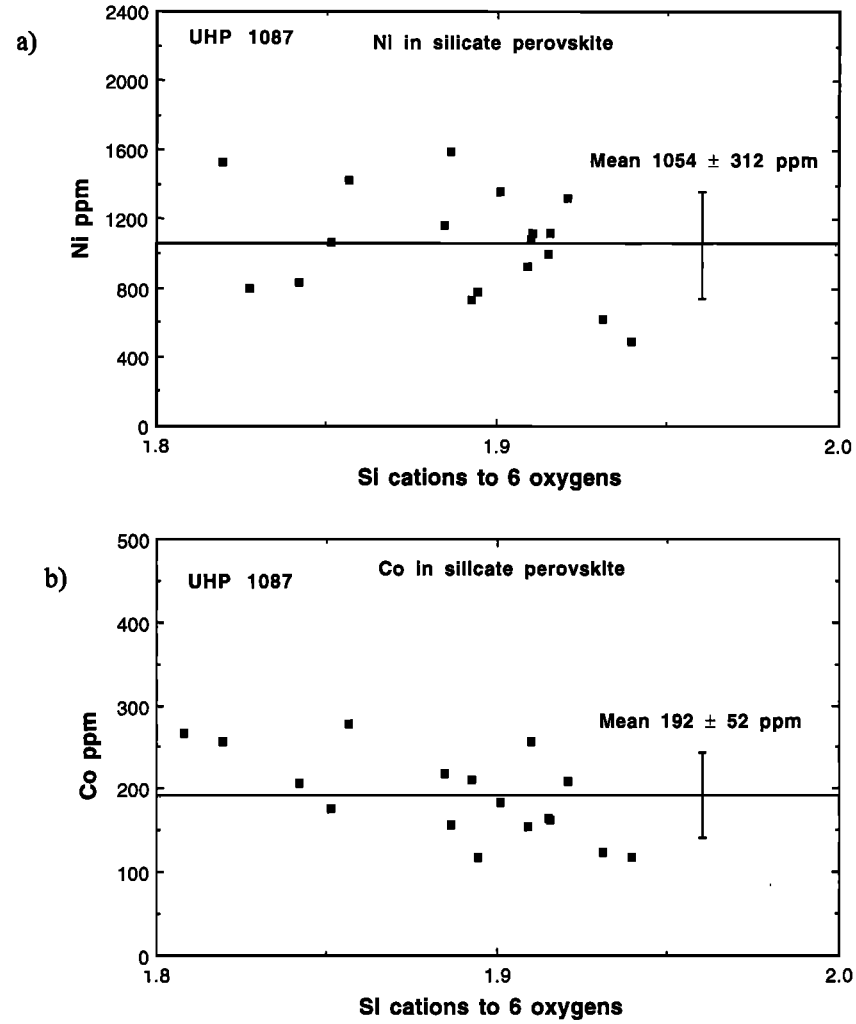

Figure 4. (a) Ni and (b) Co in perovskite. There is no apparent correlation with Si.

$$\underset{\text{metal}}{M} + x/4\ O_2 = \underset{\text{oxide (or silicate)}}{MO_{x/2}} \quad (2)$$

where x is the effective valence state of M in its oxide component. A simple expedient is to use the partitioning behavior of one element, usually Fe for convenience, to define fO_2:

$$\underset{\text{metal}}{Fe} + 1/2\ O_2 = \underset{\text{oxide (or silicate)}}{FeO} \quad (3)$$

[see, e.g., *O'Neill*, 1992]. Subtraction of (3) from (2) to eliminate O_2 gives the two element distribution reaction:

$$\underset{\text{metal}}{x/2\ Fe} + \underset{\text{oxide}}{MO_{x/2}} = \underset{\text{oxide}}{x/2\ FeO} + \underset{\text{metal}}{M} \quad (4)$$

which is independent of fO_2. The two element distribution coefficient $KD^{met/ox}_{M\text{-}Fe}$ is defined as:

$$KD^{met/ox}_{M\text{-}Fe} = (X^{met}_{M} / X^{ox}_{MOx/2}) / (X^{met}_{Fe} / X^{ox}_{FeO})^{x/2} = D^{met/ox}_{M} / (D^{met/ox}_{Fe})^{x/2} \quad (5)$$

The two element distribution coefficient is related to the thermodynamic equilibrium constant, $K^{met/ox}_{M\text{-}Fe}$, by the introduction of activity coefficients, such that

$$K^{met/ox}_{M\text{-}Fe} = KD^{met/ox}_{M\text{-}Fe} (\gamma^{met}_{M} / \gamma^{ox}_{MOx/2}) / (\gamma^{met}_{Fe} / \gamma^{ox}_{FeO})^{x/2} \quad (6)$$

where

$$RT \ln (K^{met/ox}_{M\text{-}Fe}) = -\Delta G^\circ = -\Delta H^\circ + T\Delta S^\circ - \int \Delta V^\circ dP \quad (7)$$

Where R is the gas constant T is temperature in kelvins. This suggests that measured values of the two element distribution coefficients might be fitted to an equation of the form

$$\ln KD^{met/ox}_{M\text{-}Fe} = a/T + b + cP/T \quad (8)$$

where a, b and c are constants.

For the practical purpose of doing a mass balance, it is a simple matter to calculate the required metal/oxide distribution coefficient at any desired value of $D^{met/ox}_{Fe}$:

$$D^{met/ox}_{M} = (D^{met/ox}_{Fe})^{x/2} KD^{met/ox}_{M\text{-}Fe} \quad (9)$$

This relationship can therefore be used to extrapolate values of $D^{met/ox}_{Fe}$ measured at a particular concentration of FeO in the oxide (or silicate) to that appropriate for modeling the equilibrium between the metal now in the Earth's core and mantle. Its use is also necessary to normalize experiments with

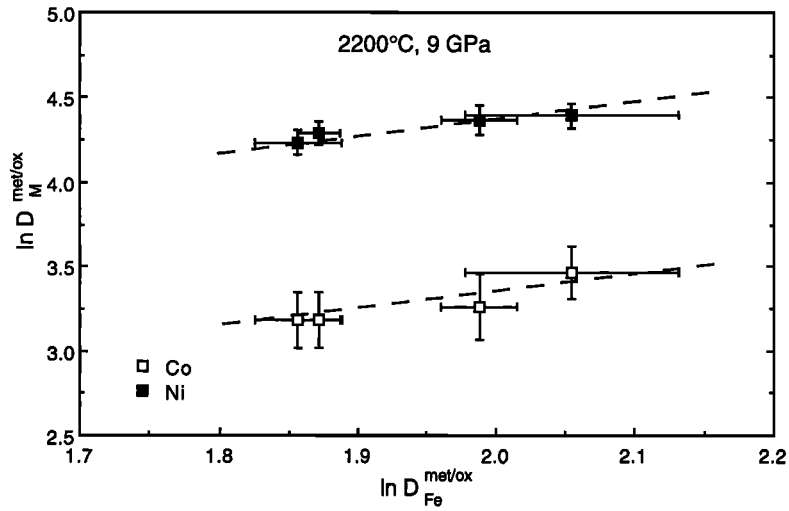

Figure 5. Distribution coefficient $D_{Ni}^{met/ox}$ and $D_{Co}^{met/ox}$ versus $D_{Fe}^{met/ox}$ for all runs at 9 GPa, 2200°C. The slope of the correlation is 1 within experimental error (dashed lines), indicating that both Ni and Co share the same valence state as Fe in the magnesiowüstite (2+).

different metal or oxide/silicate compositions to a common level, if one wishes meaningfully to compare experiments done, for example, at different T-P conditions.

A potential problem is that the effective valence state x of M in the oxide component $MO_{x/2}$ must be known. One reason for the special importance of Ni and Co in siderophile element geochemistry is that these two elements can safely be assumed to have $x = 2$ at all relevant conditions. This is confirmed in the present study (Figure 5). Other reasons are described as follows.

1. Ni and Co have cosmochemical volatilities almost identical to Fe under all likely solar nebular conditions [e.g., *Grossman*, 1972], so they can be assumed to be present in the bulk Earth in strictly chondritic proportions relative to Fe and to each other,

2. Ni and Co, as well as Fe, are compatible in the solid silicates and oxides of the mantle, which results in their chemical potentials, hence bulk metal/silicate (±oxide) distribution coefficients, not being much affected by the extent of partial melting (unlike highly incompatible elements, see, e.g., *O'Neill*, [1991a, p. 1147]). The same geochemical property of compatibility in the major mantle phases also means that their primitive mantle abundances are very accurately known [e.g., *O'Neill and Palme*, 1997; *McDonough and Sun*, 1995].

It should thus be a primary requirement that any model of core formation in the Earth, should be able to explain adequately the mantle abundances of Co and Ni.

The experimentally observed values of $KD_{Co\text{-}Fe}^{met/ox}$ and $KD_{Ni\text{-}Fe}^{met/ox}$

Table 4. Thermochemical Data Used for the Calculation of the Partitioning of Fe, Ni and Co Between Magnesiowüstite and Liquid Fe-Ni-Co Metal at High Temperatures and 0 GPa

Reactions	Free Energy, J/mol	References
$Fe+0.5\ O_2$="FeO"	-274000+70.3T	*Chase et al.* [1985]
$Co+0.5\ O_2$=CoO	-277720+212.0T-15.62TlnT	and
$Ni+0.5\ O_2$=NiO	-248060+129.2T-4.90TlnT	*O'Neill and Pownceby* [1993]
	Solution Models	
Liquid metal*	$G^{ex}=-9312X_{Co}X_{Fe}-1752X_{Co}X_{Fe}(X_{Co}-X_{Fe})+1331X_{Co}X_{Ni}+(-18379+6.039T)X_{Fe}X_{Ni}+(9228-3.546T)X_{Fe}X_{Ni}(X_{Fe}-X_{Ni})$	
Magnesiowüstite solid solution	$RT\ln\gamma_{FeO} = W_{Fe\text{-}Mg}(X_{Mg})^2$ $RT\ln\gamma_{CoO} = W_{Co\text{-}Mg}(X_{Mg})^2+W_{Co\text{-}Fe}(X_{Fe})^2+(W_{Co\text{-}Mg}+W_{Co\text{-}Fe}-W_{Mg\text{-}Fe})X_{Mg}X_{Fe}$ $RT\ln\gamma_{NiO} = W_{Ni\text{-}Mg}(X_{Mg})^2+W_{Ni\text{-}Fe}(X_{Fe})^2+(W_{Ni\text{-}Mg}+W_{Ni\text{-}Fe}-W_{Mg\text{-}Fe})X_{Mg}X_{Fe}$	
Parameter	Value, J/mol	References
$W_{Fe\text{-}Mg}$	7600+1.6T	*H.St.C. O'Neill et al.* (manuscript in preparation, 1997)
$W_{Co\text{-}Mg}$	4500	*Seifert and O'Neill* [1987]
$W_{Ni\text{-}Mg}$	700	*Seifert and O'Neill* [1987]
$W_{Co\text{-}Fe}$	3200	*Aukrust and Muan* [1963]

* from Fernández Guillermet [1989].

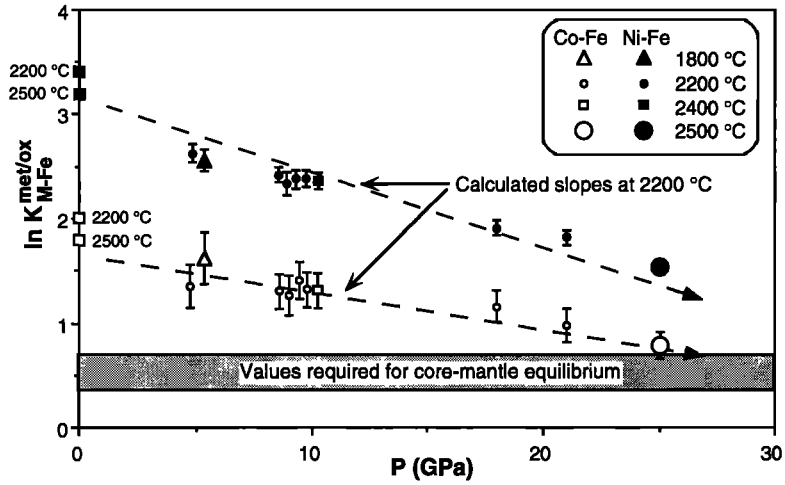

Figure 6. Experimentally observed values of distribution coefficient $KD^{met/ox}_{Ni-Fe}$ and $KD^{met/ox}_{Co-Fe}$, together with calculated values at 1 bar from (12) and (13) using the data of Table 4. The calculated values appear higher than what would be expected from a linear extrapolation of the experimental data, for reasons which are not known. Also indicated are estimates of the pressure dependences of $KD^{met/ox}_{Ni-Fe}$ and $KD^{met/ox}_{Co-Fe}$ calculated from zero-pressure molar volume data (see text for details).

The amounts by which Ni and Co are depleted relative to chondritic levels in the present Earth's upper mantle are nearly the same, so that the mantle has an almost chondritic Ni/Co ratio [e.g., O'Neill, 1991b]. The region of values of $KD^{met/ox}_{Ni-Fe}$ and $KD^{met/ox}_{Co-Fe}$ that would be required to achieve these depletions at the upper mantle's present abundance of Fe is indicated by the stippled area.

are plotted as a function of pressure in Figure 6 for the range of 5 to 25 GPa. Values of $KD^{met/ox}_{Co-Fe}$ and $KD^{met/ox}_{Ni-Fe}$ can also be calculated at 1 bar using available thermodynamic data extrapolated to high temperatures (summarized in Table 4) via (6) and (7).

Figure 6 shows several interesting features. Temperature has a small effect on the partitioning equilibria at the high temperatures of our experiments, in good agreement with the expectation from thermodynamic calculation using the data in Table 4. At constant temperature, the values of $KD^{met/ox}_{Co-Fe}$ and $KD^{met/ox}_{Ni-Fe}$ both decrease with increasing pressure, with the decrease in $KD^{met/ox}_{Ni-Fe}$ being somewhat greater than that in $KD^{met/ox}_{Co-Fe}$. The partitioning data were fitted by least squares regression, weighted according to the observed uncertainties, to an expression of the form of (8), to give

$$\ln KD^{met/ox}_{Co-Fe} = 3270/T + 0.24 - 66\,P/T \quad (10)$$

and

$$\ln KD^{met/ox}_{Ni-Fe} = 1286/T + 2.34 - 132\,P/T \quad (11)$$

where P is in gigapascals and T is in kelvins. The reduced chi-square values of the regressions are 0.15 and 0.6, respectively, indicating that the uncertainties in the Co and Ni analyses may perhaps have been overestimated. The actual values of the small temperature dependences in these equations are not well constrained by the data because of the limited range of temperatures covered (2073 to 2773 K) when these are considered as reciprocal temperatures, the quantity important for partitioning thermodynamics.

The magnitudes of the pressure dependences are in good agreement with those estimated using the approximation

$$\int \Delta V^{\circ} dP = \Delta V^{\circ}_{(2000\ K,\ 1\ bar)} P \quad (12)$$

i.e., ignoring compressibilities, which are not well known for liquid metals. A temperature of 2000 K was adopted as a compromise between the temperature range covered by the experiments and the temperature range over which volumes have been measured. We use molar volumes for NiO and CoO at 298 K, 1 bar of the pure solid oxides (10.972 and 11.658 cm^3/mol, respectively, from H. St. C. O'Neill, unpublished measurements, 1992), but for stoichiometric FeO, we use the partial molar volume obtained from "FeO"-MgO solid solutions synthesized in equilibrium with Fe metal, at $X_{Mg} > 0.7$. of 12.33 cm^3/mol (H. St. C. O'Neill, unpublished measurements, 1992). Thermal expansions of the oxides were taken from *Touzelin* [1974, 1978]. Data for liquid metals are from *Smithells* [1976]. We calculate $\Delta V^{\circ}_{(2000\ K,\ 1\ bar)} = 0.5$ cm^3/mol for the Co-Fe exchange reaction compared with the observed value of 0.5 ± 0.2 cm^3/mol from (10) and 1.2 cm^3/mol for the Ni-Fe exchange reaction compared with the observed value of 1.1 ± 0.1 cm^3/mol from (11).

The values of $KD^{met/ox}_{Co-Fe}$ and $KD^{met/ox}_{Ni-Fe}$ extrapolated to 1 bar from the regressions of the experimental data (see (10) and (11)) can be compared with those calculated using the thermodynamic data of Table 4. To do so, it is necessary to simplify the compositions of the magnesiowüstite phase by projection onto the (Mg,Fe,Co,Ni)O quaternary (i.e., ignoring the relatively small amounts of Ti, Cr, and Si), and of the liquid metal by projection onto the Fe-Ni-Co ternary systems (i.e., ignoring O, Cr, and Si). At 2200°C, the thermodynamic data predict ln $KD^{met/ox}_{Co-Fe} = 2.02$ versus 1.57 from (10) and ln $KD^{met/ox}_{Ni-Fe} = 3.43$ versus 2.86 from (11). That the discrepancies are nearly the same for both equilibria (0.45 and 0.57, respectively, corresponding to free

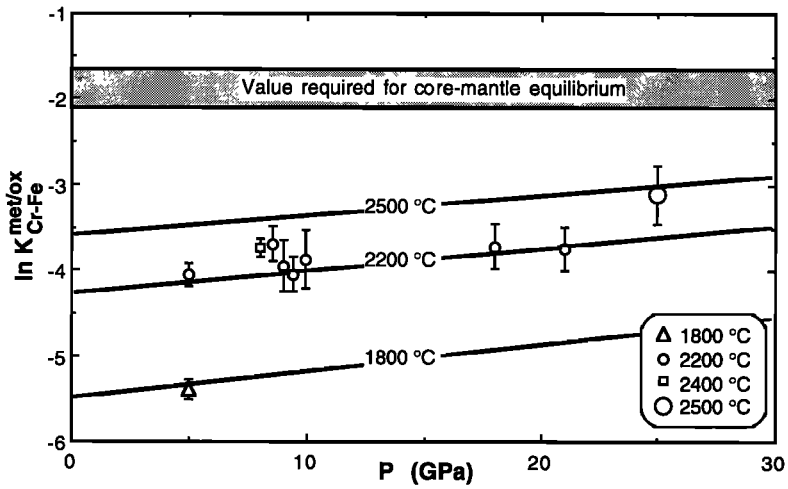

Figure 7. Experimentally determined values of ln $KD^{met/ox}_{Cr-Fe}$ (= ln ($D^{met/ox}_{M}/(D^{met/ox}_{Fe})^{3/2}$) plotted as a function of pressure. The value of $KD^{met/ox}_{Cr-Fe}$ required for core-mantle equilibrium (stippled area) would only be reached at pressure/temperature conditions well in excess of 2500°C/30 GPa.

energies, RT ln ($K_{observed}/K_{calculated}$), of 9.2 and 11.7/kJ mol^{-1}) indicates the possibility of errors in the thermodynamic data associated with Fe, i.e., either the data for the free energy of formation of FeO or the activity composition relations for MgO-FeO solid solutions (or both). The magnitude of the discrepancies is much larger than the sum of the uncertainties in the thermodynamic data in the temperature range in which the latter were measured (uncertainties in all quantities are probably < 0.2 kJ mol^{-1} at temperatures below ~1500 K, suggesting the net uncertainty should be less than ± 0.5 kJ in calculated values of RT ln K). Either the extrapolation to higher temperatures is in error or the simplification made by projecting compositions into the simple systems is unjustified. Either way, this is a point requiring further study.

4.2. Partitioning of Cr Between Magnesiowüstite and Liquid Fe-rich Metal

In runs other than the "low temperature" run UHP1027 (1800°C, 5 GPa), more than half the Cr in the original liquid metal quenches out into the blobs. Thus failure to reintegrate the quenched metal composition correctly (e.g., by overlooking the blob material) would result in a considerable underestimation of the siderophile tendencies of Cr at very high temperatures.

Unfortunately, the range of redox states covered in these experiments is too small to establish the valence state of Cr in the magnesiowüstite. We assume that it is 3+, since the amount of Cr^{2+} entering magnesiowüstite in the system MgO-Cr-O in equilibrium with Cr metal (i.e., at much more reducing conditions this study) is minimal [*Li et al.*, 1995]. This is expected from the known crystal chemical properties of Cr^{2+} which favors highly distorted crystallographic sites and not the perfectly symmetrical octahedral sites of magnesiowüstite, which are, however, favorable for Cr^{3+}.

With the assumption that Cr has a valence of 3+ in magnesiowüstite, values of ln $KD^{met/ox}_{Cr-Fe}$ (where $KD^{met/ox}_{Cr-Fe}$ = $D^{met/ox}_{Cr}/(D^{met/ox}_{Fe})^{3/2}$, from (5) were calculated for each run and are plotted in Figure 7. Regression of these data to (8) gives

$$\ln KD^{met/ox}_{Cr-Fe} = -15710/T + 2.07 + 64P/T \quad (13)$$

where T is in kelvins and P in gigapascals. Ignoring possible errors in temperature and pressure and using the uncertainties in $D^{met/ox}_{Cr}$ and $D^{met/ox}_{Fe}$ calculated from the uncertainties given in Table 3, the reduced chi-square for the regression is 0.84. Unlike $KD^{met/ox}_{Ni-Fe}$ and $KD^{met/ox}_{Co-Fe}$, $KD^{met/ox}_{Cr-Fe}$ is quite a strong function of temperature. The temperature dependence is also illustrated in Figure 7.

4.3. Partitioning of Fe, Co, Ni and Cr and Core Mantle Equilibrium in the Earth

Magnesiowüstite solid solution is the second most abundant phase in the lower mantle (i.e., below 670 km or at > 24 GPa pressure) and would comprise about 15% of the lower mantle, assuming pyrolitic bulk composition. This magnesiowüstite has molar Fe/(Fe+Mg) ≈ 0.15 for a pyrolite bulk composition, the exact composition depending on the silicate perovskite chemistry, [*Wood and Rubie*, 1996], and is a main reservoir for Ni and Co. For Ni, taking $D^{ox/pvsk}_{Ni}$ = 5 (by weight) at high temperatures and a primitive mantle abundance of 1860 ppm, implies a Ni content in the magnesiowüstite of about 6000 ppm or X_{NiO} = 0.005.

Using primitive mantle abundances of Fe and Ni from *O'Neill and Palme* [1997] (see also *McDonough and Sun*, [1995]), taking the mass of the core to be 0.32 the mass of the Earth M_E, and assuming that the core consists of Fe, Ni, and the light component (effectively all other elements), a mass balance for Ni and Fe between core and mantle can be arranged as follows:

$Fe_{core} = 0.32\,M_E\,(1-c_{Ni}-c_{LE})$

$Ni_{core} = 0.32 M_E\,c_{Ni}$

$Fe_{mantle} = 0.68\,M_E \times 6.37/100$

$Ni_{mantle} = 0.68\,M_E \times 1860/10^6$

Bulk Earth (Fe/Ni) = $(Fe_{core} + Fe_{mantle})/(Ni_{core} + Ni_{mantle})$
= 17.2 (the chondritic ratio)

We assume the concentration of the light element in the core c_{LE} is 10%. This yields an implied concentration of Ni in the core c_{Ni} of 5.3 wt %. Hence the values of $D^{core/mantle}_{Fe}$ and $D^{core/mantle}_{Ni}$ required for core/mantle equilibrium are 13.3 and 28.6, respectively, and the required value of $KD^{met/ox}_{Ni-Fe}$ is 2.1. The mass balance for Co (chondritic Fe/Co = 360, 102 ppm Co in the primitive mantle) gives $KD^{met/ox}_{Co-Fe} \approx 1.9$.

The abundance of Cr in the mantle is as well known as Ni or Co and is 2520 ppm [*O'Neill and Palme*, 1997]; it is therefore depleted relative to its chondritic abundance by a factor of 0.42, Mg-normalized. This depletion requires $D_{Cr}^{core/mantle} = 3.3$. Cr is probably enriched in magnesiowüstite relative to coexisting perovskites in natural systems by a factor of 2 [*Kesson and Fitz Gerald*, 1991], but this enrichment depends on the details of the perovskite chemistry (as shown, for example, in this study; see Figure 3c). We assume, for the sake of argument, that the abundance of Cr in the magnesiowüstite in a mantle of pyrolite composition is approximately 4500 ppm. Hence the required value of $D_{Cr}^{met/ox}$ is 2 (weight percent basis) and of $KD_{Cr\text{-}Fe}^{met/ox}$ is ~0.15 for core-mantle equilibrium.

The values of $KD_{Co\text{-}Fe}^{met/ox}$, $KD_{Ni\text{-}Fe}^{met/ox}$, and $KD_{Cr\text{-}Fe}^{met/ox}$ required for core mantle equilibrium according to these mass balances are indicated by the shaded regions in Figures 6 and 7. Clearly, none of the required values can be satisfied by P, T conditions within the range of these experiments (i.e., down to the top of the lower mantle). Metal extraction at temperatures at which the lower mantle is partially molten would lower the required values of all three distribution coefficients slightly, as Fe is likely to be less compatible in magnesiowüstite relative to silicate melt than Co or especially Ni and Cr. This would make the discrepancy worse.

Extrapolation of the present results via (10) and (11) shows that the mass balances for Co-Ni-Fe could be satisfied at 37 GPa and 2260 K. However, at these conditions, (13) gives $KD_{Cr\text{-}Fe}^{met/ox}$ = 0.02 versus the required value of ~ 0.15. Substantially higher temperatures seem to be needed to achieve the observed depletion of Cr in the mantle (e.g., 3360 K at 37 GPa), at which the values of $KD_{Co\text{-}Fe}^{met/ox}$ and $KD_{Ni\text{-}Fe}^{met/ox}$ predicted by eqns. (10) and (11) would be too low. More definitive conclusions clearly require further experimental work at still higher temperatures and pressures.

4.4. Partitioning of Ti Between Magnesiowüstite and Liquid Fe-rich Metal

Values of $D_{Ti}^{met/ox}$ in all experiments are extremely low. Since Ti partitions preferentially into silicate phases compared with magnesiowüstite (e.g., into $MgSiO_3$-perovskite in UHP1081 and UHP1087), the presence of additional silicate phases in real mantle systems will reduce the siderophile propensities of Ti further still. We thus come to a conclusion that is opposite of that of *Ringwood and Hibberson* [1991]: that Ti does not show any significant siderophile tendencies in compositionally realistic mantle systems at relevant fO_2, and that Ti is less siderophile than Si, not more.

The behavior of Ti during high T-P metal silicate equilibria is potentially of great importance, in that the observed relative abundance of Ti in the upper mantle is within ± 20% of other refractory lithophile elements such as Ca, Al, and the heavy rare earth elements [*McDonough and Sun*, 1995; *O'Neill and Palme*, 1997]. Thus any conditions that substantially partition Ti from mantle silicate into Fe-rich metal can be excluded from consideration in modeling core formation. From these experiments, it appears that a modest amount of Si partitioning into the metal of the Earth's core would still be consistent with the mantle's observed chondritic Ca/Ti ratio.

4.5. The Solubility of O in Liquid Fe-rich Metal

The present experiments provide the first quantitative measurements of the solubility of oxygen in Fe-rich metal in equilibrium with the kind of Mg-rich compositions appropriate for modeling the chemistry of planetary mantles. The amount of oxygen dissolved in Fe-rich metal in equilibrium with silicate or oxide can be described thermodynamically by

$$\underset{\text{silicate/oxide}}{FeO} = \underset{\text{metal}}{Fe} + \underset{\text{metal}}{O} \qquad (14)$$

This relation shows that the amount of O in Fe metal is proportional to the activity of FeO in coexisting silicate or oxide; if magnesiowüstite is present, then the activity of FeO is, in turn, proportional to X_{Feo}^{ox}, the mole fraction of FeO.

In the regime of upper mantle pressures (< 25 GPa), the present experiments were conducted at higher activities of FeO than would occur (at the same P, T) during the accretion of the Earth because of lower a_{SiO2}; this is true whether an homogenous accretion scenario or any plausible heterogenous model is

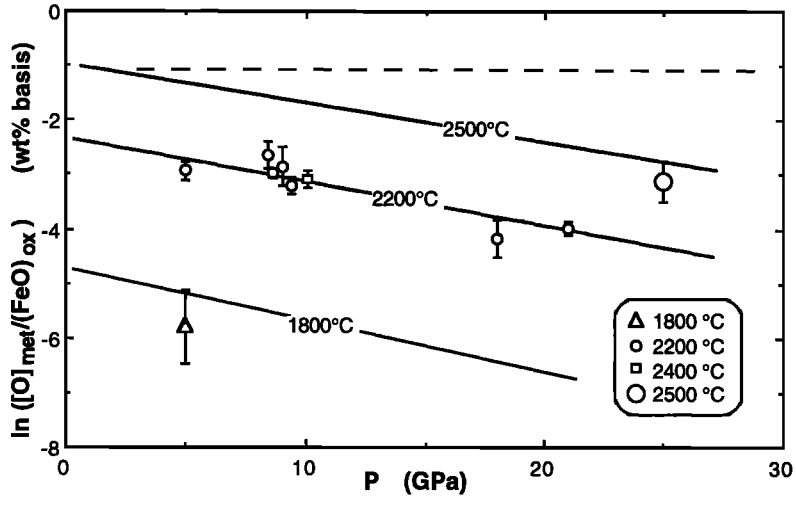

Figure 8. Solubility of O in liquid Fe-rich metal in equilibrium with magnesiowüstite as a function of pressure and temperature. The solid lines are calculated from a least squares fit to the data, ignoring the anomalous result of UHP984. The solubility of O in liquid Fe-rich metal decreases with increasing pressure. The dashed line indicates 8 wt % O (the amount needed to produce a 10% density deficit in the core according to *Poirier* [1994]) in equilibrium with magnesiowüstite with $X_{Feo}^{ox} = 0.15$ (24 wt% FeO).

assumed [e.g., *O'Neill*, 1991a,b]. Nevertheless, the amount of FeO found to dissolve in Fe-Ni metal is an order of magnitude less than that required to account for the core's density deficit. At 25 GPa (top of the lower mantle), where magnesiowüstite becomes a stable phase in cosmochemically reasonable mantle compositions, our experimental phase assemblage of magnesiowüstite plus perovskite duplicates that of the mantle. At X^{ox}_{Feo} = 0.08, we find only 0.6±0.2 wt % O in metal. Extrapolating to the X^{ox}_{Feo} appropriate to present upper mantle Mg/Fe ratios ($X^{ox}_{Feo} \approx 0.15$) would give ~1 wt % O, well below the 8 wt % needed according to *Poirier* [1994].

Possible effects of temperature and pressure on the solubility of O in liquid Fe-rich metal in equilibrium with magnesiowüstite are shown in Figure 8. It is expected from theoretical considerations that the solubility of O should increase markedly with increasing temperature [*Ohtani et al.*, 1984; *Kato and Ringwood*, 1989], as found here, for example, by the large increase in solubility between runs UHP1027 (1800°C, 5 GPa) and UHP986 (2200°C, 5 GPa). However, run UHP984 (2400°C, 9 GPa) does not show any increased solubility over the several runs at 2200°C at the same pressure.

The effect of pressure is illustrated well by the series of runs at 2200°C (5 to 21 GPa). Contrary to the findings of *Ohtani et al.* [1984], *Kato and Ringwood* [1989], and *Ringwood and Hibberson* [1990] on the binary system Fe-FeO, involving equilibrium between liquid metal and a liquid oxide phase, we observe a decrease in the solubility of O with increasing pressure at constant temperature and mole fraction of FeO in coexisting magnesiowüstite. Part of the reason for this apparent discrepancy with the earlier studies is that the partial molar volume of FeO in solid magnesiowüstite is less than the partial molar volume of FeO in the FeO-rich liquid that coexists with Fe metal in the binary system investigations, as discussed by *Ohtani et al.* [1984]. Quantitatively, however, this change in molar volume should not be sufficient to reverse the sign of the pressure dependence (as shown by *Ohtani et al.* [1984, Figure 7]).

Excluding the anomalous datum from UHP984, the remaining nine data can be well fit to an empirical equation with the form of (8), to give

$$\ln([O]_{metal}/(FeO)_{oxide}) = -30760/T + 10.1 - 197\,P/T \qquad (15)$$

where $[O]_{metal}$ and $(FeO)_{oxide}$ are the concentrations in weight percent of oxygen in the metal and FeO in magnesiowüstite, respectively.

The densities of metallic-like melts in the system Fe-S-O have been directly measured by *Kaiura and Toguri* [1979] between 1200°C and 1350°C using an Archimedean technique and an alumina bob. The results suggest a remarkably high partial molar volume (i.e., low density) for liquid FeO dissolved in Fe-S liquids, e.g., ~19 cm^3/mol at 1350°C (the experimental results are difficult to interpret exactly, as the composition of the Fe-S-O melts were modified during the experiments by gas emission). This compares with a partial molar volume of 12.9 cm^3/mol for solid FeO in magnesiowüstite at the same temperature. Thus these direct density measurements independentally support a strong decrease of the solubility of O in metallic melts with pressure.

The decrease in solubility of O with increasing pressure has important implications for our understanding of the composition of the core. It implies that although a fairly large amount of O could be dissolved into Fe-rich metal under upper mantle conditions at very high temperatures (e.g., >3000 K), there would be a tendency for this O subsequently to exsolve out at higher pressures, following metal segregation and core formation. Our finding also has implications for speculations regarding possible core/mantle interactions across the D″ layer [e.g., *Knittle and Jeanloz*, 1991; *Goarant et al.*, 1992]. In conclusion, these experiments seem to rule out that sufficient O is able to dissolve in Fe-Ni metal to account for the core's 10% density deficit.

4.6. The Solubility of Si in Liquid Fe-Rich Metal

The highest pressure experiments attempted in this study, at 25 GPa (UHP1081 and UHP1087), contain both the highest levels of Si in quenched matrix metal (~ 1 wt %) and the highest amounts (recalculated) of total Si in the original liquid metal (1.4 wt % in UHP1087). Nevertheless, this amount is still an order of magnitude less than that required to account for the core's 10% density deficit (18 wt % Si according to *Poirier* [1994].

The solubility of Si in Fe-rich metal is described by

$$\underset{\text{silicate/oxide}}{SiO_2} = \underset{\text{metal}}{Si + O_2} \qquad (16)$$

and thus depends on the activity of silica (a_{SiO2}) in the system and the oxygen fugacity. In these experiments, the oxygen fugacity is given by

$$\underset{\text{metal}}{2\,Fe + O_2} = \underset{\text{magnesiowüstite}}{2\,FeO} \qquad (17)$$

Thus for a given a_{SiO2}, the amount of Si in Fe metal should vary in inverse proportion to the square of the mole fraction of FeO in coexisting magnesiowüstite:

$$[Si]_{metal} \approx k_{Si}\,(a_{SiO2})/(\,X^{ox}_{Feo}\,)^2 \qquad (18)$$

where k_{Si} is an equilibrium constant. Since the 25 GPa experiments contain $MgSiO_3$-rich perovskite, the experimental phase assemblage mimicks that at the top of the Earth's lower mantle, and buffers a_{SiO2} at approximately the correct value for modeling the present mantle's composition (the substitution of relatively minor elements such as Fe, Al, Ti, etc., in the perovskite has a minor effect on a_{SiO2} and may be ignored). The value of X^{ox}_{Feo} in UHP1087 is 0.08, which is about half that appropriate for the presently observed upper mantle bulk Mg #; consequently, the amount of Si in liquid Fe-rich metal in equilibrium with the present upper mantle composition at 25 GPa and 2500°C would only be ~ 0.4 wt %.

Equation (18) predicts that, in the context of a heterogenous accretion model for the Earth, 5% Si in Fe-rich metal would be achieved at $X^{ox}_{Feo} \cong 0.04$. This would correspond to a mantle Mg# of ~ 0.98, which is reasonable for the first 80% of material accreting to the Earth in the context of a heterogeneous accretion model [*O'Neill*, 1991a, b].

In the experiments below 25 GPa, the lack of an identified magnesiosilicate phase means that a_{SiO2} is not known, although the presence of magnesiowüstite necessarily implies lower values of a_{SiO2} than those in the Earth's mantle. In peridotitic and other cosmochemically pertinent compositions at temperatures somewhat below the liquidus, the a_{SiO2} changes with pressure according to a series of reactions in the subsystem MgO-SiO_2, the main ones of which at 2500 K are (in order of increasing pressure)

$$\underset{\text{olivine}}{Mg_2SiO_4} + SiO_2 = \underset{\text{orthopyroxene}}{Mg_2Si_2O_6} \qquad (19)$$

$$\underset{\text{wadsleyite}}{Mg_2SiO_4} + SiO_2 = 2\,\underset{\text{majorite}}{MgSiO_3} \qquad (20)$$

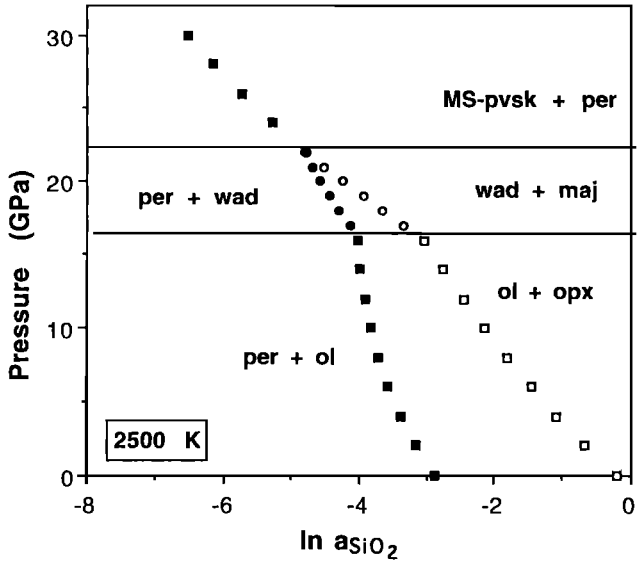

Figure 9. Calculated values of $\ln(a_{SiO2})$, where a_{SiO2} is activity of silica, at 2500K, relative to a standard state of b quartz at the pressure of interest, as defined by phase assemblages in the model system MgO-SiO_2. All thermodynamic data are from *Saxena et al.* [1993]. Open squares denote phase assemblages with mantle Mg/Si ratios; solid square denote phase assemblages with excess MgO, a condition which most of these experiments are probably near. The two conditions become identical above 23 GPa. Note that these solid phase assemblages are not stable with respect to melt at low pressures and 2500 K, but in this regime, the calculation is still useful for illustrative purposes. Some minor phase stability fields have been omitted for simplicity, e.g., at 2500 K; the transition from olivine to wadsleyite in Mg_2SiO_4 happens (according to the thermochemical data) to occur at almost the same pressure as that of orthopyroxene to majorite in $MgSiO_3$; the absence of ringwoodite (γ-Mg_2SiO_4), a relatively low temperature phase, is as predicted by the thermochemical data.

$$\underset{\text{magnesiowüstite}}{MgO} + SiO_2 = \underset{\text{perovskite}}{MgSiO_3} \qquad (21)$$

The values of a_{SiO2} referenced to a standard state of β quartz at the pressure of interest and 2500 K are shown in Figure 9, calculated from the thermodynamic data of *Saxena et al.* [1993]. Also shown in Figure 9 are the calculated values of a_{SiO2} in each pressure regime defined by the equilibrium of the appropriate magnesiosilicate with MgO, which may be taken to be the upper limit of the actual values of a_{SiO2} in the experiments below 25 GPa. Hence these experiments provide only lower limits on the solubility of Si in the coexisting metal. However, the experiments at 9 GPa and 2200°C, which were performed using different starting mixes with varying levels of SiO_2 , resulted in constant levels of Si in the metal of the run products, demonstrating that a_{SiO2} was controlled by saturation with a magnesiosilicate phase, although this was unobserved (a possibility is an intergranular melt phase in the MgO capsule). The mean amount of Si in the metal of four experiments at 9 GPa and 2200°C (UHP981, UHP1069, UHP1180 and UHP1183) is 0.31 ± 0.03 wt %.

Equation (18) shows that the results for the solubility of Si obtained at lower a_{SiO2}, in equilibrium with MgO (as in the experiments), can be translated to mantle a_{SiO2} using

$$[Si]^{mantle}_{metal} = [Si]^{expt}_{metal} \, (a_{SiO_2})^{mantle} / (a_{SiO_2})^{expt} \qquad (22)$$

where $(a_{SiO2})^{mantle}$ and $(a_{SiO2})^{expt}$ may be obtained at 2500 K from Figure 9 as a function of pressure. Thus at 9 GPa and 2200°C, the solubility of Si in a mantle in equilibrium with olivine plus orthopyroxene is calculated to be approximately 6 times that observed in our experiments if these are, in fact, saturated with olivine, i.e., ~ 1.8 wt %. This is similar to the value constrained experimentally by the perovskite/magnesiowüstite equilibrium at 25 GPa and 2500°C. These results therefore indicate that the solubility of Si in metal probably decreases with increasing pressure when the activity of silica is buffered by realistic mantle assemblages, at least down to pressures equivalent to the top of the lower mantle.

Figure 9 further illustrates that the value of a_{SiO2} defined by $MgSiO_3$-perovskite plus MgO (the lower mantle assemblage) decreases quite markedly with increasing pressure at pressures above 25 GPa, such that we may expect the decrease in the solubility of Si in metal with increasing pressure inferred from our experiments to continue to even greater pressures.

5. The Problem of the "Light Component" in the Earth's Core

5.1 Can S, Si or O alone comprise the "Light Component"?

These results for the solubility of O and Si in Fe-rich metal in equilibrium with mantle-like compositions exacerbate the difficulties in solving the longstanding conundrum of what the identity of the light component in the Earth's core may be. That so many elements have been proposed as candidates (specifically, S, O, Si, C and H; see *Poirier* [1994]) should not obscure the fact that none satisfies all the constraints on the subject. The most important chemical constraints derive from the observation that the Earth's mantle is heavily depleted in all the cosmochemically volatile elements, including those that are lithophile and whose depletion in the bulk Earth may therefore be estimated reliably from their mantle abundances (e.g., Na, K, B, and the halides [*McDonough and Sun*, 1995; *O'Neill and Palme*, 1997]. Moreover, the observed degree of depletion of these lithophile volatile elements correlates empirically very well with semiquantitative measurements of their cosmochemical volatility, i.e., the magnitude of their depletions in the ordinary chondrite and carbonaceous chondrite meteorites or with their calculated "50% condensation temperatures" from the solar nebula [e.g., *Kargel and Lewis*, 1993; *O'Neill and Palme*, 1997]. This shows the depletion to be of cosmochemical origin.

Thus although S has often been proposed as being a suitable candidate for the light component in the core from the point of view of its physical-chemical properties [e.g., *Murthy and Hall*, 1970; *Ahrens*, 1982], its cosmochemical volatility is such that its abundance in the bulk Earth is probably insufficient for enough to be present in the core to account for the density deficit [e.g., *Ringwood*, 1977]. Sulfur is certainly cosmochemically more volatile than Na or K. Even in the enstatite chondrite meteorites, which formed under conditions of unusually high fS_2 (and which thus exhibit many geochemical features such as chalcophile behavior of Ca, Ti, and REE, which are not seen in the chemistry of the Earth's mantle), S is more depleted than Na and K. Sulfur should therefore be more depleted than Na and K in the bulk Earth, limiting the amount of S in the core to less than 6 wt % or about half the amount required for the density deficit. *Dreibus and Palme* [1996] have recently argued that the depletion factor

for S in the bulk Earth is more realistically modeled using the relative abundance of Zn, in the mantle: this approach yields an upper limit of ~1.7 wt % S in the core.

The volatility argument would also seem to rule out H, C, and N. It has not been possible to construct a cosmochemical scenario in which the required amounts of these highly volatile elements could be condensed, without also postulating that other, somewhat less volatile elements (including S) would be nearly fully condensed.

The volatility objection to S prompted *Ringwood* [1977] to propose O as the light element. Although O is only slightly soluble in liquid Fe near its melting point at 1 atmosphere pressure, *Ringwood* [1977, 1984] demonstrated experimentally that sufficient O can become soluble at higher (superliquidus) temperatures in the simple system Fe-O to make the candidacy of O a finite possibility. However, the present results in a more geologically relevant system show that the amounts of O that can dissolve in liquid Fe-rich metal in equilibrium with magnesiowüstite are nearly an order of magnitude below the required levels.

There are, in any case, several additional cosmochemical problems concerning the hypothesis that O is the light element in the Earth's core that were not addressed by *Ringwood* [1977, 1984]. The first problem concerns the volatility of O itself. The condensation behavior of O in a solar nebula environment follows a pattern different than that of all other elements. Some O is among the first material to condense with the refractory elements (e.g., the O in Al_2O_3), and more condenses with Mg and Si. For most purposes, this O can be considered as remaining bound to the lithophile element with which it condenses and would not be available for partitioning into the core. It is only at considerably lower temperatures that more O condenses by oxidation of Fe metal, forming the FeO component of silicates. Significantly, this oxidation begins near the condensation temperature of S [*Grossman and Larimer*, 1974; *Saxena and Eriksson*, 1986]. Thus available O (i.e., that O which is not inextricably bound up in nonsiderophile oxide components such as Al_2O_3, CaO, SiO_2, and MgO) is, in fact, cosmochemically more volatile than S. The conclusion is that if one must propose a volatile element for the light component, then S at least has the merit of being the least volatile; but even S is too volatile.

This leaves Si. One superficially attractive feature of having Si in the core is that Si is depleted in the Earth's mantle compared with its presumed solar abundance (as in CI chondrites) when normalized to the refractory lithophile elements. This has led some authors to propose that the "missing" Si is in the core [e.g., *MacDonald and Knopoff*, 1958]. However, analysis of the meteoritic data shows that the core needs only to contain 5 wt % Si to reconcile the bulk silicate Earth Mg-Si-Al ratios with the carbonaceous chondrite Mg-Si-Al trend [*O'Neill*, 1991b; see also *O'Neill and Palme*, 1997, Figure 17]. Any more Si in the core would result in bulk Earth Mg/Si and Al/Si ratios that are unlike those of any other known solar system composition. It should be remembered that Si is not very effective at reducing the density of liquid Fe, so that *Poirier* [1994] estimates that no less than 18 wt % Si is needed for a 10% density deficit.

Another problem in supposing that there is enough Si in the core to contribute significantly to the core's density deficit is the mass balance for the oxygen associated with Si. This constraint arises because Si condenses from the solar nebula into silicates [e.g. *Grossman and Larimer*, 1974], i.e., as an SiO_2 component; for example, in Mg_2SiO_4 (olivine). The amount of Si partitioning into Fe-rich metal under all reasonable solar nebular T-fO_2 conditions is inconsequential. (This low Si is mainly a consequence of the solubility of Si in Fe-rich metal being a sensitive function of temperature; any significant solubility would require too high temperature for any plausible solar nebular pressure). The enstatite chondrites, which record oxidation conditions considerably more reducing than the canonical solar nebula, only have 2% Si in metal, e.g., *Zhang et al.* [1995]. Thus it seems reasonable to assume that material accreting to the early Earth initially condensed with nearly all Si in the oxidized state (i.e., as an SiO_2 component). With initially all Si as SiO_2 and all Fe in the metallic state, the dissolution of Si into Fe-rich metal may be described by

$$SiO_2 + 2\,Fe = Si + 2\,FeO \qquad (23)$$

If the Earth was a closed system, to achieve 18 wt % Si in Fe-rich metal would liberate enough oxygen, given the relative masses of core and mantle (0.32 and 0.68 M_E respectively), to produce a mantle concentration of FeO of 43 wt %

$$FeO \approx 2 \times 18\ wt\ \% \times (71.85/28.06) \times (0.32/0.68) = 43\ wt\ \% \qquad (24)$$

where 71.85 and 28.06 are the molecular weights of FeO and Si, respectively. This is 5 times the present observed abundance of FeO in the Earth's mantle and indeed implies higher bulk Earth Fe contents than are cosmochemically reasonable. Of course, the buildup of FeO in the silicate would bring the reaction to a halt before this level was reached (Le Chatelier's principle).

Open system loss of O from the primitive Earth is perhaps not impossible, but it is unlikely. For example, loss of O as an H_2O component as part of a general H degassing requires an enormous source of H, presumably a massive primitive atmosphere of solar composition. The persistence of such an atmosphere seems unlikely in view of recent results that have dated core formation in the Earth to >50 m.y. after collapse of the solar nebula, as deduced from the W-Hf isotopic system [*Lee and Halliday*, 1995]. A similar late date is probable from the isotopic composition of terrestrial Pb [*Galer and Goldstein*, 1996].

The important conclusion is that from the chemical view, none of the cosmochemically abundant light elements appears able to account for the mystery light component in the core, at least when considered individually. It therefore seems logical to inquire whether a combination of Si and O as light elements could provide an answer to this dilemma.

5.2. Both Si and O in the Core?

The cosmochemical and geochemical objections would seem to be removed if both Si and O could simultaneously become soluble in Fe-rich metal, in sufficient amounts. For example, consider if Si and O in the ratio given by the stoichiometry of SiO_2 could be dissolved in Fe-rich metal. If the 10% density deficit can be satisfied by a linear combination of 8.2 wt % of O alone and 18 wt % of Si alone (i.e., wt % O = 8.2-(8.2/18) wt % Si), dissolution of stoichiometric SiO_2 requires 5.9 wt % O and 5.0 wt % Si. This is exactly the amount of Si required to reconcile the bulk silicate Earth composition with the carbonaceous chondrite Mg-Si-Al trend [*O'Neill and Palme*,1997]. The amount of SiO_2 needed to be lost from the mantle would be 5 wt %, which is only about 11% of the present amount. Actually, the ratio of Si to O dissolved in liquid Fe can, in principle, have any value, and we shall refer to the dissolved component as Si_xO. A value of x slightly greater than 0.5 is the most appropriate for avoiding conflict with the oxygen mass balance constraint discussed above.

Unfortunately, evidence from the practice of steelmaking does not favor the simultaneous dissolution of Si and O in liquid Fe. In fact, Si was widely used as a deoxygenating agent in steelmaking, and, consequently, the physical chemistry of the equilibrium between Si and O in liquid Fe is rather well understood, at least at atmospheric pressure and temperatures up to 2000 K [e.g., *Ward*, 1962].

Following standard metallurgical practice [*Ward*, 1962], it is convenient to represent the equilibrium between silica and the silicon and oxygen in molten iron as

$$[Si]_{l\ wt\%} + 2\ [O]_{l\ wt\%} = SiO_2 \quad (25)$$

where the brackets refer to Si and O dissolved in liquid Fe. The standard state for Si and O is 1 wt % dissolved in the Fe. The equilibrium constant is

$$K_{Si\text{-}O} = a_{SiO2}/[c_{Si}][c_O]^2 \quad (26)$$

which, from experimental data on silica saturated slags ($a_{SiO2} \approx 1$), has the value of

$$\log K_{Si\text{-}O} = 29150/T - 11.01 \quad (27)$$

[*Gokcen and Chipman*, 1952; *Chipman et al.*, 1954]. The value of this equilibrium constant has been found to remain independent of c_{Si} up to 15 wt% but the presence of a solvus between liquid Fe and liquid FeO in the system Fe-FeO at temperatures below 2500°C [*Kato and Ringwood*, 1989; *Ringwood and Hibberson*, 1990] indicates that some dependency on c_O would be observed at levels greater than those investigated by the metallurgists (which are generally less than 1 wt%). For the sake of argument, this complication will be ignored.

The amounts of Si and O in molten Fe predicted by (26) and (27) at silica saturation, extrapolated slightly in temperature from the original measurements (which extend to 2000 K) are presented in Figure 10, together with the amounts proposed by *Poirier* [1994] as being needed to satisfy the core density deficit. The nature of the equilibrium constant $K_{Si\text{-}O}$ is obviously such that the solubilities of Si and O are largely mutually exclusive (which is, of course, the reason why silicon is used as a deoxygenating agent), and it is evident that significant solubility of Si with O at the Si/O ratios needed to satisfy the oxygen mass balance would not be achieved at atmospheric pressure, except by extrapolating the trends shown in Figure 10 to excessively high temperatures (which, in any case, is not a solution, as the Si and O would precipitate out upon cooling).

The question, then is, does this mutual exclusivity persist at higher pressures? In some preliminary experiments on the simple join Fe-SiO_2 at 1900°C and 16 GPa, *Ringwood and Hibberson* [1991] did demonstrate a solubility of ~1 wt% SiO_2 in liquid Fe coexisting with stishovite and speculated that more may dissolve at higher T and P. However, the activity of FeO (hence fO_2) was not controlled in these experiments, and the effects of lower activities of SiO_2 in actual mantle compositions was not addressed.

In order to compare our experimental data collected at different pressures, temperatures, and values of a_{SiO2}, in Figure 11 we plot the equilibrium constant $K_{Si\text{-}O}$ (see (26)) for the combined solubilities of Si and O as a function of pressure using values of a_{SiO2} calculated, as in Figure 9 from *Saxena et al.* [1993]. Also plotted is the value of $K_{Si\text{-}O}$ calculated at 1 bar from the metallurgical literature (see (27)). The experiments at 18 and 22 GPa are probably at lower activity of silica than that which would be defined by the presence of wadsleyite (no silicate phase was found in these runs), hence the plotted values of $K_{Si\text{-}O}$ should be taken as being upper limits only. Taking this into account, it appears that there may be a slight decrease of $K_{Si\text{-}O}$ with pressure, but realistically, the data are not accurate enough to quantify this. Nevertheless, two important observations can still be made.

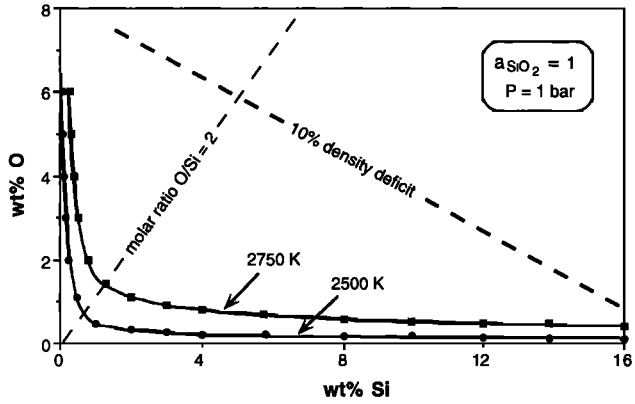

Figure 10. The mutual dependence of the solubilities of Si and O in liquid Fe at 1 bar from the steel-making literature (see (26) and (27)). The solubilities are drawn for $a_{SiO2}=1$. The solubilites of Si and O are largely mutually exclusive, which is why Si was used as a deoxygenating agent in steel making. Also shown (dashed line) is the combined level of Si and O solubilities needed to account for a 10% density deficit in the Earth's outer core, according to *Poirier* [1994].

1. The high pressure experimental data extrapolate back reasonably toward the 1 atm values, showing that the solubilities of Si and O at high pressure are of similar magnitude to those observed during steelmaking processes and that there is no evidence of a major change in the chemistry of Fe-Si-O metals at pressures to 25 GPa.

2. Any decrease in $K_{Si\text{-}O}$ with pressure is relatively modest and of comparable magnitude to the decrease in a_{SiO2} when buffered by mantle phases (Figure 9). For example, above 23 GPa, the value of $d(\ln(a_{SiO2}))/dP$ buffered by MgO + $MgSiO_3$ (perovskite) is, from *Saxena et al.* [1993], about -0.20 GPa^{-1}. In Figure 11, we have drawn lines of this slope from the calculated 1 atm values of $K_{Si\text{-}O}$ to show that $d(\ln(K_{Si\text{-}O})/dP$ is about this magnitude. Thus there is no evidence that the effect of pressure will be to enhance significantly the combined solubilities of Si and O in core-forming metal.

6. Conclusions

High pressures corresponding to those in the Earth's lower mantle can have a major effect on metal/silicate partitioning relations. Nevertheless, the high T, P partitioning data for Fe,Ni, Co, and Cr obtained here show that the mantle abundances of these elements cannot be explained by equilibration of metal with mantle material to pressures corresponding to the top of the lower mantle in the Earth. A currently favored model of Earth accretion and core formation envisages that metal/silicate segregation takes place in Mars-sized or smaller planetary protoliths [*Stevenson*, 1990; *Taylor and Norman*, 1990]. It has been suggested that cores of such differentiated protoliths should combine during accretion without reequilibrating with the mantle silicate [*Benz and Cameron*, 1990] Such a scenario is only possible if the mantle's abundances of the siderophile elements were then set by

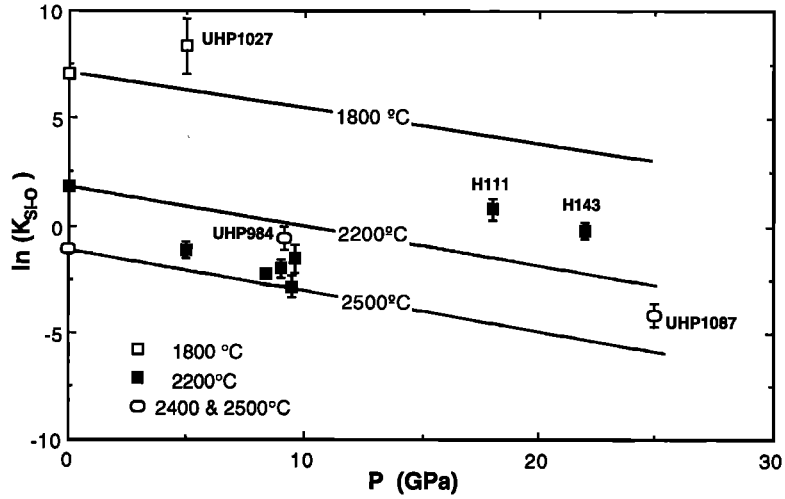

Figure 11. Values of $K_{Si\text{-}O}$ (the "solubility product" for Si and O, defined in (26)) as a function of pressure. The data have been normalized to a_{SiO2}=1 using thermochemical data for the model MgO-SiO_2 system from *Saxena et al.* [1993] and assuming that the experiments are buffered by MgO and the appropriate silicate phase (forsterite, wadsleyite, or $MgSiO_3$-perovskite). Runs with silica activities lower than assumed (e.g., probably H111 and H143) would be expected to plot at higher values of $K_{Si\text{-}O}$. Values plotted at zero pressure are calculated from thermodynamic data [*Ward*, 1962]. Error bars on the experimental data are from the 1s observed errors in Si and O contents of the metals (Table 3) and take no account of experimental errors in pressure or tempreature, or the uncertainty in calculated a_{SiO2}. The precision of the data is insufficient to quantify the effect of pressure on $K_{Si\text{-}O}$, but clearly it cannot be large and positive (it is, in fact, probably negative). The important point for constraining core formation models is that the change of $\ln(K_{Si\text{-}O})$ with pressure is likely to be the same order as the change in $\ln(a_{SiO2})$ with pressure above 23 GPa , which is about 0.2 GPa-1. Lines of this slope (i.e., $d(\ln(K_{Si\text{-}O})/dP = 0.2$ GPa-1) are shown for the sake of argument. It appears unlikely that pressure increases the combined solubilities of Si and O in Fe-rich metal sufficiently enough to account for the light component in the core.

late stage accretion of a more oxidized component [e.g., *O'Neill*, 1991b].

The experimental results presented here also show that for reasonable presentday mantle compositions, at pressures from zero to those appropriate for the top of the lower mantle and at temperatures extending into the mantle superliquidus regime, neither O nor a combination of O with Si can dissolve in liquid Fe-rich metal in sufficient amounts to account for the presumed density deficit in the Earth's outer core. This raises severe difficulties in accounting for sufficient light component to explain the core's 10% density deficit relative to pure Fe-Ni alloy.

We summarize the objections to the various light component candidates, as discussed in this paper as follows. (1) Sulfur is cosmochemically too volatile to have accreted in sufficient amounts [e.g., *Ringwood*, 1977; *Dreibus and Palme*, 1996]. (2) C, H, N, and available O are cosmochemically even more volatile than S. (3) The experimental work presents an arguement that, contrary to earlier suggestions [e.g.,*Ringwood*, 1977, 1984], O is not sufficiently soluble in Fe-rich metal in equilibrium with cosmochemically reasonable compositions of appropriate Mg #. (4) Since Si condenses as an SiO_2 component, its subsequent partitioning into Fe-rich metal releases a prohibitively large amount of excess O. (5) Owing to the antithetical dependence of the solubilities of Si and O on oxygen fugacity, the combined solubilies of Si and O are too low for both elements simultaneously to contribute significantly to the density deficit.

At present, there appear to be several ways in which this dilemma might be resolved. The lack of quantitative experimental measurements on the solubility of Si and O at the pressures of the present core mantle boundary (130 GPa) still leaves open the possibility that a light component of Si plus O might have been established by processes operating at such pressures, if a suitable mechanism for delaying metal/silicate segregation during the Earth's accretion can be found. Alternatively, it is certainly possible that the core is not a "clean system" [*Stevenson*, 1981]; a stew of light elements, each in an amount that is the upper limit given by the various cosmochemical arguments discussed above (e.g., perhaps ~2% of S, O, and Si, plus some C, and possibly others) would add up to about half that required, according to *Poirier* [1994], to account for the presumed 10% density deficit. This then raises the question of how robust such a estimate of the density deficit really is; in other words, how well known are the equations of state of liquid Fe and Fe-S-Si-O alloys at core pressures? In evaluating such a query, it is pertinent to note that the melting point of Fe at core pressures was recently revised downward by ~2000 K [*Boehler*, 1993], removing one of the other reasons (apart from density) for postulating a light component in the Earth's outer core, namely, that an antifreeze seems necessary if there is not too high a temperature jump across the core mantle boundary [*Stevenson*, 1990].

Acknowledgments. We would like to thank Nick Ware for his considerable help with the electron microprobe analyses and François Guyot, Carl Agee, and an anonymous reviewer for helpful reviews.

References

Ahrens, T.J., Constraints on core composition from shock-wave data, *Philos Trans. R. Soc. London. Ser. A, 306*, 37-47, 1982.

Aukrust, E. and A. Muan, Activities of components in oxide solid

solutionsæthe systems CoO-MgO, CoO-MnO, and CoO-'FeO' at 1200°C., *Trans. Metall. Soc. AIME, 227*, 1378-1380, 1963.

Benz W., and A. G. W. Cameron, Terrestrial effects of the giant impact, in *Origin of the Earth*, edited by H.E. Newsom and J.H. Jones, pp. 61-67, Oxford Univ. Press, New York, 1990.

Birch, F., Density and composition of mantle and core, *J. Geophys. Res., 69*, 4377-4388, 1964.

Boehler, R., Temperatures in the Earth's core from melting-point measurements of iron at high static pressures, *Nature, 363*, 534-536, 1993.

Canil, D., Stability of clinopyroxene at pressure-temperature conditions of the transition region, *Phys. Earth Planet. Inter ., 86*, 25-34, 1994a.

Canil, D., An experimental calibration of the Ni in garnet geothermometer with applications, *Contrib. Mineral. Petrol., 117*, 410-420, 1994b.

Chase, M.W., Jr., C.A. Davies, J.R. Downey, Jr., D.J. Frurip, R.A. McDonald, and A.N. Syverud, JANAF thermochemical tables, third ed. *J. Phys. Chem. Ref. Data, 14*, suppl. 1, 1985.

Chipman, J., J.C. Fulton, N. Gokcen, and G.R. Caskey, Activity of silicon in liquid Fe-Si and Fe-C-Si alloys, *Acta Metall., 2*, 439-450, 1954.

Darken, L. S., and R. W. Gurry, *Physical Chemistry of Metals*, McGraw-Hill, New York, 1953.

Dreibus, G., and H. Palme, Cosmochemical constraints on the sulfur content in the Earth's core, *Geochim. Cosmochim. Acta, 60*, 1125-1130, 1996.

Falloon, T.J., and D.H. Green, Anhydrous partial melting of MORB pyrolite and other peridotite compositions at 10 kbar: Implications for the origin of primitive MORB glasses, *Mineral. Petrol., 37*, 181-219, 1987.

Fei, Y., H.-K. Mao and B.O Mysen, Experimental determinatyion of element partitioning and calculation of phase relations in the MgO-FeO-SiO2 system at high pressure and high temperature, *J. Geophys. Res., 96*, 2157-2169, 1991.

Fernandez Guillermet, A., Assessing the thermodynamics of the Fe-Co-Ni system using a Calphad predictive technique, *CALPHAD Publ. 13 (*1), 1-22, 1989.

Freer, R., Bibliography self diffusion and impurity diffusion in oxides, *J. Mater. Sci., 15*, 803-824, 1980.

Galer, S.J.G., and, S.L. Goldstein, Influence of accretion on lead in the Earth, in *Earth Processes Reading the Isotopic Code, Geophys. Monog. Ser.*, vol. 95, edited by A. Basu and S. Hart., pp. 75-98, AGU, Washington, D.C., 1996.

Goarant, F., F. Guyot, J. Peyronneau,. and J.-P. Poirier, High-pressure and high-temperature reactions between silicates and liquid iron alloys, in the diamond anvil cell, studied by analytical electron microscopy, *J. Geophys. Res., 97*, 4477-4487, 1992.

Gokcen, N.A. and J. Chipman, Silicon-oxygen equilibrium in liquid iron, *Trans. Am. Inst. Min. Mettall. Pet., Eng., 194*, 171-181, 1952.

Green, D.H., Experimental melting studies on a model upper mantle composition at high pressure under water-saturated and water-undersaturated conditions, *Earth Planet. Sci. Lett., 19*, 37-53, 1973.

Grossman, L., Condensation in the primitive solar nebula, *Geochim. Cosmochim. Acta. 36*, 597-619, 1972.

Grossman, L., and J.W., Larimer, Early chemical history of the solar system, *Rev. Geophys., 12*, 71-101, 1974.

Hofmann, A.W., Diffusion in natural silicate melts: A critical review, in *Physics of Magmatic Processes*, edited by R.B Hargraves, pp. 385-418, Princeton Univ. Press, Princeton, N.J., 1980.

Irifune, T., Absence of an aluminous phase in the upper part of the Earth's lower mantle, *Nature 370*, 131-133, 1994.

Ito, E., E. Takahashi, and, Y. Matsui, The mineralogy and chemistry of the lower mantle: An implication of the ultrahigh-pressure phase relations in the system MgO-FeO-SiO_2, *Earth Planet. Sci. Lett., 67*, 238-248, 1984.

Ito, E., K. Morooka, O. Ujike, and T. Katsura, Reactions between molten iron and silicate melts at high pressure: Implications for the chemical evolution of Earth's core, *J. Geophys. Res., 100*, 5901-5910, 1995.

Johnson, K.T.M., and I. Kushiro, Segregation of high pressure partial melts from peridotite using aggregates of diamond: A new experimental approach, *Geophys. Res. Lett., 19*, 1703-1706, 1992.

Kaiura, G. H., and J. M. Toguri, Densities of the molten FeS, FeS-Cu_2S and Fe-S-O systems - Utilizing a bottom-balance Archimedean technique. *Can. Metall. Q., 18*, 155-164, 1979.

Kargel, J. S., and J. S. Lewis, The composition and early evolution of the Earth, *Icarus, 105*, 1-25, 1993.

Kato, T,. and A.E. Ringwood, Melting relationships in the system Fe-FeO at high pressures: Implications for the composition and formation of the Earth's core, *Phys. Chem. Miner., 16*, 524-538, 1989.

Kesson, S.E. and Fitz Gerald, J.D., Partitioning of MgO, FeO, NiO, MnO and Cr_2O_3 between magnesian silicate perovskite and magnesiowüstite: Implications for the origin of inclusions in diamond and the composition of the lower mantle, *Earth Planet. Sci. Lett., 111*, 229-240, 1991.

Knittle, A., and R. Jeanloz, Simulating the core-mantle boundary: Results of experiments at high-pressure and temperatures, *Science, 251*, 1438-1443, 1991.

Lee, D.-C. and A.N. Halliday, Hafnium-tungsten chronometry and the timing of terrestrial core formation, *Nature, 378*, 771-774, 1995

Li, J.-P., l, H. St.C. O'Neill, and F. Seifert,. Subsolidus phase relations in the system MgO-SiO_2-Cr-O in equilibrium with metallic Cr, and their significance for the petrochemistry of chromium, *J. Petrol., 36*, 107-132, 1995.

Malavergne, V., F. Guyot, Y Wang, and I. Martine, Partitioning of nickel, cobalt and manganese between silicate perovskite and periclase: a test of cystal field theory at high pressure, *Earth Planet. Sci. Lett., 146*, 499-509, 1997.

MacDonald, G.J. and L. Knopoff, On the chemical composition of the outer core. *Geophys. J. Royal Astron. Soc. 1*, 284-297, 1958.

McCammon, C., Perovskite as a possible sink for ferric iron in the lower mantle, *Nature, 387*, 694-696, 1997.

McDonough, W.F., and S.-S. Sun, The composition of the Earth, *Chem. Geol., 120*, 223-253, 1995.

McFarlane, E.A., M.J. Drake, and D.C. Rubie, Element partitioning between Mg-perovskite, magnesiowüstite, and silicate melt at conditions of the Earth's mantle, *Geochem. Cosmochim. Acta, 58*, 5161-5172, 1994.

Murthy, V.R., and H.T. Hall, The chemical composition of the Earth core: Possibility of sulfur in the core, *Phys. Earth Planet. Inter., 2*, 276-282, 1970.

Ohtani, E., and A.E. Ringwood, Composition of the core, I, Solubility of oxygen in molten iron at high temperatures, *Earth Planet. Sci. Lett., 71*, 85-93, 1984.

Ohtani, E., A.E. Ringwood, and, W. Hibberson, Composition of the core, II, Effect of high pressure on solubility of FeO in molten iron, *Earth Planet. Sci. Lett., 71*, 94-103, 1984.

Ohtani, E., T. Kato and E. Ito, Transition metal partitioning between lower mantle and core materials at 27 GPa, *Geophys. Res. Lett., 18*, 85-88, 1991.

O'Neill, H.St.C., The origin of the Moon and the early history of the Earth: A chemical model, 1, The Moon, *Geochim. Cosmochim. Acta., 55*, 1135-1157, 1991a.

O'Neill, H.St.C., The origin of the Moon and the early history of the Earth: A chemical model, 2, The Earth, *Geochim. Cosmochim. Acta, 55*, 1159-1172, 1991b.

O'Neill, H.St.C., Siderophile elements and the Earth's formation, *Science, 257*, 1282-1285, 1992.

O'Neill, H.St.C. and H. Palme, Composition of the silicate Earth: Implications for Accretion and core formation, in *The Earth's Mantle: Structure, Composition and Evolution - the Ringwood Volume*, pp. 3-126, Cambridge Univ. Press, New York, 1997.

O'Neill, H.St.C. and M.I. Pownceby, Thermodynamic data from redox reactions at high temperatures, I, An experimental and theoretical assessment of the electrochemical method using stabilized zirconia electrolytes, with revised values for the Fe - "FeO", Co-CoO, Ni-NiO and Cu-Cu_2O oxygen buffers, and new data for the W-WO_2 buffer, *Contrib. Mineral. Petrol., 114*, 296-314, 1993.

Palme, H., and H.St.C. O'Neill, Formation of the Earth's core, *Geochim. Cosmochim. Acta., 60*, 1106-1108, 1996.

Poirier, J.-P., Light elements in the Earth's outer core: A critical review, *Phys. Earth Planet. Inter., 85*, 319-337, 1994.

Richardson, F.D., *Physical Chemistry of Melts in Metallurgy*, Academic Press, San Diego, Calif., 1974.

Ringwood, A. E., The chemical evolution of terrestrial planets, *Geochim. Cosmochim. Acta, 30*, 41-104, 1966.

Ringwood, A.E., Composition of the core and implications for origin of the earth, *Geochem. J., 11*, 111-135, 1977.

Ringwood, A.E., The Earth's core: Its composition, formation and bearing upon the origin of the Earth, *Proc. R. Soc. London, A, 395*, 1-46, 1984.

Ringwood, A.E. and W. Hibberson, The system Fe-FeO revisited, *Phys. Chem. Miner., 17*, 313-319, 1990.

Ringwood, A.E., and W. Hibberson, Solubilities of mantle oxides in molten iron at high pressures and temperatures: Implications for the composition and formation of Earth's core, *Earth Planet. Sci. Lett., 102*, 235-251, 1991.

Rubie, D.C., S. Karato, H.Yan, and H.St.C. O'Neill, Low differential

stress and controlled chemical environment in multi-anvil high pressure experiments. *Phys. Chem. Miner.*, *20*, 315-322, 1993a.

Rubie, D.C., C.R. Ross, II, M.R. Carroll, and S.C. Elphick, Oxygen self-diffusion in $Na_2Si_4O_9$ liquid up to 10 GPa and estimation of high pressure viscosities, *Am. Mineral.*, *78*, 574-582, 1993b.

Saxena, S.K. and G, Eriksson, Chemistry and formation of the terrestrial planets, in *Chemistry and Physics of the Terrestrial Planets, Adv. in Phys. Geochem.*, Vol. 6, 30-105, edited by S.K. Saxena, pp. 30-105, Springer Verlag, Berlin, 1986.

Saxena, S.K., N. Chatterjee, Y. Fei, and G. Shen, *Thermodynamic Data on Oxides and Silicates*, Springer-Verlag, New York, 1993.

Seifert, S., and H.St.C. O'Neill, Experimental determination of activity-composition relations in Ni_2SiO_4-Mg_2SiO_4 and Co_2SiO_4-Mg_2SiO_4 olivine solid solutions at 1200 K and 0.1 MPa and 1573 K and 0.5 GPa, *Geochim. Cosmochim. Acta.*, *51*, 97-104, 1987.

Smithells, C.J. (Ed), *Metals Reference Book*, 5th ed., Butterworths, London, 1976.

Stevenson, D.J., Models of the Earth's core, *Science*, *214*, 611-619, 1981.

Stevenson, D.J., Fluid dynamics of core formation, *Origins of the Earth*, edited by H.E. Newsom and J.H. Jones, pp. 231-249, Oxford Univ. Press, New York, 1990.

Taylor, S.R. and M.D. Norman, Accretion of differentiated Planetesimals to the Earth, in *Origins of the Earth*, edited by H.E. Newsom and J.H. Jones, pp. 29-43, Oxford Univ. Press, New York, , 1990.

Touzelin, B., High temperature X-ray determination of iron monoxide lattice parameters under controlled atmosphere. Decomposition of iron monoxide between 25 and 570°C, *Rev. Int. Hautes Temp. Réfract*, *11*, 219-230, 1974.

Touzelin B., Etude par diffraction des rayons x à haute température, en atmospere controlée, des oxydes de cobalt et de nickel, *Rev. Int. Hautes Temp. Réfract*, *15*, 33-41, 1978.

Ward, R.G., *An Introduction to the Physical Chemistry of Iron and Steel Making*, Edward Arnold, London, 1962.

Ware, N.G., Combined energy-dispersive-wavelength-dispersive quantitative electron microprobe analysis, *X Ray Spectrom.*, *20*, 73-79, 1991.

Wood, B. J., and J. Nicholls, The thermodynamic properties of reciprocal solid solutions, *Contrib. Mineral. Petrol*, *66*, 389-400, 1978.

Wood, B. J., and D. C. Rubie, The effect of alumina on phase transformations at the 660-kilometer discontinuity from Fe-Mg partitioning experiments, *Science 273*, 1522-1524, 1996.

Zanda, B., M. Bourot-Denise, C. Perron, and R.H. Hewins, Origin and metamorphic redistribution of silicon, chromium and phosphorus in the metal of chondrites, *Science*, *265*, 1846-1849, 1994.

Zhang, Y., P. H. Benoit, and D. W. G. Sears, The classification and complex thermal history of the enstatite chondrites, *J. Geophys. Res. 100*, 9417-9438, 1995.

D. Canil, School of Earth and Ocean Sciences, University of Victoria, PO Box 1700, Victoria, British Columbia, Canada V8W 2Y2. (e-mail: dcanil@uvic.ca)

H.St.C. O'Neill, Research School of Earth Sciences, Australian National University, Canberra ACT 0200, Australia. (e-mail: hugh.oneill@anu.edu.au).

D.C. Rubie, Bayerisches Geoinstitut, Universität Bayreuth, 95440 Bayreuth, Germany. (e-mail: dave.rubie@uni-bayreuth.de)

(Received July 30, 1996; revised April 23, 1997;
accepted September 11, 1997.)